

Project Number: CM-RWT-0610

AN EXAMINATION OF THE PHYSICO-CHEMICAL  
FIRE RETARDANT MECHANISM OF BURN-X™ IN WOOD

Major Qualifying Project Report

submitted to the Faculty of the

WORCESTER POLYTECHNIC INSTITUTE

in partial fulfillment of the requirements for the

Degree of Bachelor of Science

by

---

**Parth BHUPTANI**

Date: April 26, 2007

Approved:

---

**Professor R. W. Thompson**

---

**Professor J. R. Barnett**

1. fire retardant
2. wood, pine
3. TG, thermogravimetry
4. pyrolysis

## **Acknowledgments**

I would like to thank the following members of the WPI community for their assistance and support in the completion of this Major Qualifying Project:

*Professor R. W. Thompson, Advisor*

*Professor J. R. Barnett, Co-Advisor and Melbourne guide*

I would also like to thank the Australia's Commonwealth Scientific and Research Organization (CSIRO) for the opportunity to work on this project, and letting me use their equipment. In particular, I would like to thank the following members of the CSIRO CMIT community who were instrumental in the achievement of this project:

*Donavan Marney*

*Glenn Bradbury*

*Ashley Bicknell*

*Gregg Griffin*

*Lee Russell*

*Terra Soegeng*

## **Abstract**

Pine was treated with a fire retardant agent called Burn-X, which is mainly an aqueous solution of calcium cations, to impart flame retardancy. Fire retardant treated and untreated samples were subjected to differential thermal analysis (DTA) and thermogravimetry (TG) in air and nitrogen environments to study their thermal behaviors. From the resulting data, kinetic parameters for different stages of thermal degradation were obtained following the method of Broido. Cone calorimetry and Fourier-Transform infrared (FTIR) spectroscopy were also conducted to understand mechanistic properties of both materials. Activation energies were found to decrease, and higher residual masses were found in the treated samples, which indicated an improvement in the flame retardancy of the treated wood.

# Table of Contents

<b>1</b>	<b>INTRODUCTION .....</b>	<b>7</b>
<b>2</b>	<b>BACKGROUND.....</b>	<b>10</b>
2.1	WOOD.....	10
2.1.1	<i>The Physical and Chemical Properties of Wood.....</i>	<i>10</i>
2.1.2	<i>Thermal Degradation of Wood .....</i>	<i>11</i>
2.2	AN OVERVIEW OF FIRE RETARDANTS.....	14
2.2.1	<i>Fire Retardant Mechanisms.....</i>	<i>14</i>
2.2.2	<i>Physical Processes .....</i>	<i>15</i>
2.2.3	<i>Chemical Processes .....</i>	<i>15</i>
2.2.4	<i>Types of Fire Retardants.....</i>	<i>16</i>
2.2.5	<i>Chemical Classes of Fire Retardants .....</i>	<i>17</i>
2.3	EQUIPMENT.....	19
2.3.1	<i>Cone Calorimeter .....</i>	<i>19</i>
2.3.2	<i>TGA-DTGA / DTA.....</i>	<i>24</i>
2.3.3	<i>FTIR.....</i>	<i>27</i>
2.3.4	<i>Porosimeter .....</i>	<i>30</i>
2.4	DATA COLLECTION PARAMETERS.....	33
2.4.1	<i>Heat Release Rate (HRR).....</i>	<i>34</i>
2.4.2	<i>Thermogravimetric Curves .....</i>	<i>37</i>
2.5	KINETICS.....	37
2.5.1	<i>Kinetic Parameters .....</i>	<i>38</i>
2.5.2	<i>The Broido Model.....</i>	<i>38</i>
<b>3</b>	<b>METHODOLOGY.....</b>	<b>41</b>
3.1	SAMPLE PREPARATION .....	41
3.2	CONE CALORIMETRY PILOT TESTS .....	42
3.2.1	<i>Determining the Heat flux.....</i>	<i>42</i>
3.2.2	<i>Determining Key Times .....</i>	<i>44</i>
3.2.3	<i>Pilot Test Discussion.....</i>	<i>45</i>
3.3	CONE CALORIMETER TESTING.....	46
3.3.1	<i>Liquid Nitrogen Quenching .....</i>	<i>47</i>

3.3.2	<i>Combustion Method</i> .....	49
3.3.3	<i>Pyrolysis Method in Nitrogen and Low O<sub>2</sub> environment</i> .....	57
3.4	TGA-DTSC AND FTIR.....	61
3.4.1	<i>Sample Preparation</i> .....	61
3.4.2	<i>Thermogravimetric Analysis and Infrared Spectroscopy</i> .....	63
3.5	POROSITY.....	64
<b>4</b>	<b>DATA ANALYSIS</b> .....	<b>65</b>
4.1	CONE CALORIMETER .....	65
4.2	TGA.....	65
4.3	FTIR.....	66
<b>5</b>	<b>RESULTS AND ANALYSIS</b> .....	<b>67</b>
5.1	KINETIC PARAMETERS .....	67
5.2	FTIR ANALYSIS OF GASEOUS EMISSIONS.....	75
5.2.1	<i>FTIR Data</i> .....	77
5.3	CONE CALORIMETRY .....	88
5.3.1	<i>Mass Percent</i> .....	89
5.3.2	<i>Mass Loss Rate</i> .....	90
5.3.3	<i>Heat Release Rate</i> .....	91
5.3.4	<i>Recommendations</i> .....	93
5.4	TGA-DTA .....	94
5.4.1	<i>Discussion of thermogravimetric analyses</i> .....	96
5.4.2	<i>Discussion of Burn-X treated pine</i> .....	99
<b>6</b>	<b>CONCLUSIONS</b> .....	<b>102</b>
<b>7</b>	<b>REFERENCES</b> .....	<b>104</b>
<b>8</b>	<b>APPENDIX A – BURN-X™ MSDS</b> .....	<b>104</b>

## Table of Figures

FIGURE 1: THE BURNING CYCLE OF WOOD .....	12
FIGURE 2: TYPICAL CONE CALORIMETER SETUP .....	21
FIGURE 3: CSIRO CONE CALORIMETER SCHEMATIC.....	22
FIGURE 4: CONE CALORIMETER AT CSIRO .....	23
FIGURE 5: EXTERNAL VIEW OF THE TGA-DSC .....	26
FIGURE 6: SAMPLE HOLDERS IN THE TGA-DSC APPARATUS .....	26
FIGURE 7: FTIR APPARATUS.....	29
FIGURE 8: FTIR AND TGA-DSC EQUIPMENT BEING USED IN CONJUNCTION .....	30
FIGURE 9: QUANTACHROME POROSIMETER.....	33
FIGURE 10: HEAT RELEASE RATE CURVE FOR UNTREATED TIMBER AT 25 kW M <sup>-2</sup> .....	35
FIGURE 11: HRR CURVE FOR BURN-X TREATED WOOD AT 25 kW M <sup>-2</sup> .....	36
FIGURE 14: VACUUM PRESSURE METHOD.....	42
FIGURE 15: HRR FOR 25 kW M <sup>-2</sup> SAMPLE.....	43
FIGURE 16: HRR FOR 35 kW M <sup>-2</sup> SAMPLE.....	43
FIGURE 17: LIQUID NITROGEN QUENCHING APPARATUS.....	47
FIGURE 18: WOOD SAMPLE FROM CONE BEING COOLED .....	48
FIGURE 19: CONDITIONING CABINET AT 23±2°C AND 50±5% RELATIVE HUMIDITY .....	53
FIGURE 20: LIQUID NITROGEN AND GLYCOL TANKS.....	57
FIGURE 21: UNTREATED TIMBER SAMPLES FOR TGA.....	63
FIGURE 22: TREATED TIMBER SAMPLES FOR TGA .....	63
FIGURE 23: DERIVATIVE WEIGHT LOSS CURVE FOR UNTREATED WOOD, 10°C MIN <sup>-1</sup> .....	70
FIGURE 24: COMPARISON BETWEEN RECALCULATED AND GAO'S ACTIVATION ENERGIES .....	71
FIGURE 25: MASS-LOSS FOR PYROLYSIS OF TREATED AND UNTREATED WOOD HEATED AT 7.5°C MIN <sup>-1</sup> .....	73
FIGURE 26 : MASS-LOSS FOR COMBUSTION OF TREATED AND UNTREATED WOOD HEATED AT 7.5°C MIN <sup>-1</sup> .....	74
FIGURE 27: GASES EVOLVED DURING THE COMBUSTION OF UNTREATED WOOD, OVERLAID WITH MLR.....	77
FIGURE 28: HEAT RELEASE RATE DATA OVERLAID WITH GAS EMISSION DATA .....	80
FIGURE 29: PLOT OF GASES EVOLVED DURING PYROLYSIS OF UNTREATED PINE, OVERLAID WITH MLR CURVE .....	81
FIGURE 30: PLOT OF GASES EVOLVED DURING COMBUSTION OF BURN-X TREATED PINE; OVERLAID WITH MLR... ..	84

FIGURE 31: HEAT RELEASE RATE CURVE AND GASEOUS EMISSIONS DURING COMBUSTION OF TREATED PINE.....	85
FIGURE 32: PLOT OF GASEOUS EMISSIONS FROM PYROLYSIS OF BURN-X TREATED PINE; OVERLAID WITH MLR ....	86
FIGURE 33: MASS PERCENT AS A FUNCTION OF TIME.....	89
FIGURE 34: MASS LOSS RATE AS A FUNCTION OF TIME.....	90
FIGURE 35: HEAT RELEASE RATE AS A FUNCTION OF TIME .....	92
FIGURE 36: THERMOGRAVIMETRIC PLOT FOR COMBUSTION OF UNTREATED PINE.....	95
FIGURE 37: THERMOGRAVIMETRIC PLOT FOR PYROLYSIS OF UNTREATED PINE.....	95
FIGURE 38: THERMOGRAVIMETRIC PLOT FOR COMBUSTION OF TREATED PINE.....	96
FIGURE 39: THERMOGRAVIMETRIC PLOT FOR PYROLYSIS OF TREATED PINE.....	96

## Tables

TABLE 1: BREAKDOWN OF THE COMBUSTION OF WOOD.....	13
TABLE 2: EXAMPLES OF ADDITIVE AND REACTIVE FIRE RETARDANTS, WHICH HAVE BEEN USED FOR WOOD.....	17
TABLE 3: ACTIVATION ENERGY OF COMBUSTION OF TREATED PINE AT 3 DIFFERENT HEATING RATES .....	68
TABLE 4: ACTIVATION ENERGY OF PYROLYSIS OF TREATED PINE AT 3 DIFFERENT HEATING RATES .....	68
TABLE 5: ACTIVATION ENERGY OF COMBUSTION OF UNTREATED PINE AT 3 DIFFERENT HEATING RATES.....	68
TABLE 6: ACTIVATION ENERGY OF PYROLYSIS OF UNTREATED PINE AT 3 DIFFERENT HEATING RATES.....	68
TABLE 7: ACTIVATION ENERGY DATA OF CHINESE LARCH [GAO ET AL.].....	70
TABLE 8: ACTIVATION ENERGIES RECALCULATED IN 4 PHASES.....	71
TABLE 9: CALCULATED PYROLYSIS PARAMETERS OF TREATED WOOD.....	73
TABLE 10: CALCULATED PYROLYSIS PARAMETERS OF UNTREATED WOOD.....	73
TABLE 11: CALCULATED OXIDATION PARAMETERS OF TREATED WOOD.....	75
TABLE 12: CALCULATED OXIDATION PARAMETERS OF UNTREATED WOOD .....	75
TABLE 13: GAS EMISSION DATA FOR COMBUSTION OF UNTREATED PINE .....	78
TABLE 14: GAS EMISSION DATA FOR PYROLYSIS OF UNTREATED WOOD .....	82
TABLE 15: TOTAL GAS EMISSIONS (MG G <sup>-1</sup> ).....	87

# 1 Introduction

Wood is an extensively used material and is present in myriad places in our everyday lives. Not only is wood an integral part of most structures, especially in North America and Europe, but is also the main source of furnishings found in homes, schools, and offices around the world. As a result, up to ninety percent of any given structure may contain some form of wood. The often inevitable hazards of fire make wood a very desirable material for further investigation.

It is therefore the aim of this project to examine and gain a better understanding of the physical and chemical properties of wood, and thus be able to predict more accurately the complexities of its behavior in fire. This knowledge would be useful and could be applied in the numerous disciplines involving wood; for example, the data could be helpful in evaluating the decomposition of wood in a fire scenario.

Several types of fire-retardants are commonly available today in the commercial wood-treating industry. Those commonly used are a variety of ammonium phosphates and sulfates, borax, boric acid, GUP, and zinc chloride (Holmes 1977). These materials have been tested thoroughly around the world under different conditions (Wang, et al. 2004). However, no products containing large concentrations of the calcium cation and chloride anion have undergone substantial testing. A Turkish company called Vega Kimya Ltd has developed 'Burn-X', a fire retardant which is mainly an aqueous solution of calcium cations. It is a chemical with sizeable proportions of calcium and chloride ions, and in conjunction with the Commonwealth Scientific and Industrial Research Organization (CSIRO) of Australia, testing was performed to determine the burning mechanisms of Burn-X. The Material Safety Data Sheet (MSDS) for Burn-X can be found in Appendix A.

In order to analyze wood products, the cone calorimeter was used to test the flammability of untreated and fire retardant treated wood. As Tran (1992) notes, many factors have been identified as key variables that affect the burning of wood. These include density, chemical composition, 'hardness' of wood, and moisture content. Other factors such as porosity, volatile matter content, and the char contraction factor are also considered in order to model the combustion of wood accurately.

Cone calorimeters can be used to quantify the different stages of the combustion process of wood by measuring the rate of heat release that may result from different exposure conditions. These tests yield Heat Release Rate curves, where the heat release rate is normally expressed as power per unit area exposed ( $\text{kW m}^{-2}$ ). From previous testing of untreated wood, it is known that once the initial peak heat release rate is reached, the combustion process slows down to a plateau. This is thought to be due to the formation of char on the surface that traps volatile matter within the wood, preventing significant levels of pyrolysis. However, once this relatively stable layer of char disintegrates, another peak of relatively smaller amplitude occurs as a result of the sudden release and combustion of the previously trapped volatiles.

On the other hand, using a sample treated with fire retardant behaves differently under the same conditions. Firstly, the peak heat release rate (PHRR) occurs later and at lower heat release rate. The plateau and peaks that represent the release of trapped volatiles under the char are much less pronounced.

To methodically test and analyze the process, we can consider the cases at hand separately for fire retardant treated and untreated timber. Each process can be further broken down to individual processes. Firstly, the levels of oxygen, carbon dioxide, and carbon monoxide in the flame plume can monitor the combustion efficiency, which is a function of the degree of degradation. The samples can then

be quenched by the means of liquid nitrogen. Using a volumetric sorption analyzer, the porosity and surface area of the char can be analyzed. Further analysis of the char, volatile matter content, and proximate moisture content can be evaluated using the TGA.

Finally, model development for the two cases, fire retardant treated and untreated wood was carried out. Char development analysis for the two sets was then compared and contrasted, ultimately providing more information about the behavior of wood in fires. Furthermore, different types of fire retardant woods and available coatings could also be tested to increase knowledge of materials and their behavior to add to a growing repertoire of substances.

The knowledge gained from this study could prove to be very helpful in the numerous disciplines of fire protection. For example, studies on structural integrity of wooden structure would be benefited by these results. Additionally, the results could also help engineers decide which materials and coatings are better suited to which applications.

## **2 Background**

The aim of the literature review is to clearly define the terminology related to this project and to ensure a thorough understanding of the Methodology and the data analysis sections that follow subsequently.

We start out by discussing the basics: degradation of wood when exposed to high levels of heat, an overview of fire retardants, followed by discussion of the equipment used in this investigation, namely – a cone calorimeter, a thermogravimetric analyzer, and an infrared spectrometer. Using this equipment, the heat release rate for wood was measured, which is a convenient method to quantify the various aspects of the combustion process, as well as the amounts and types of gas emitted during combustion and pyrolysis. Finally, we explore the materials tested, with and without the fire retardant treatment. Significant parts of this background information come from the CSIRO Project Report PN04.2007 by Marney, Russell, and Mann (2006).

### **2.1 Wood**

#### **2.1.1 The Physical and Chemical Properties of Wood**

Three major polymeric components make up wood: cellulose, hemicellulose, and lignin, according to Bourgois, Fang, Meier, and Rowell, in addition to small amounts of organic extractives and inorganic trace elements (Alén 2000). The polymeric components that make up the cell wall are responsible for most of the physical and chemical properties that wood exhibits. Cellulose is a long-chained, linear sugar molecule, or polysaccharide composed of glucose monomers. Glucose is a hexose or a six-carbon ring sugar, and as a cellulose polymer, it accounts for about forty to forty-five percent of the dry weight of wood (Parham, et al 1984). Wood's strength

can be attributed to the high molecular weight of the cellulose. Hemicellulose molecules are polysaccharides with lower molecular weights that contain short side chains. Mainly, they contain combinations of various five-carbon sugars (xylose and arabinose), and six-carbon sugars such as glucose, mannose, and galactose. These make up between twenty to thirty percent of the dry weight of wood (Parham, et al 1984). Lignin, a random three-dimensional network polymer, makes up between fifteen to thirty-five percent of the dry weight of wood. It is a hydrophobic, phenolic material comprised of hydroxyl- and methoxyl- substituted phenylpropane units that hold the wood (cellulose and hemicellulose) together, and is also responsible for imparting rigidity to wood (Miller 1999 and Winandy, et al 1984).

### **2.1.2 Thermal Degradation of Wood**

When exposed to a constant source of heat, wood undergoes thermal decomposition, but does not burn directly. It is rather the oxidation of the gases released (Browne 1958). Like most reactions in nature, this is not a singular process, but is in fact a combination of chemical and physical processes. A number of bonds are broken within the structure of the wood and volatile products are formed and released. As shown in Figure 3 (Grassie et al 1985), the burning process is comprised of several steps. The first stage is pyrolysis, which is caused by the heating of the wood. Products such as combustible gases, vapors, and mists are released. Char and tar are the respective solid and liquid carbon residues that result from this initial step. Gas or other volatiles may also be released during this stage; however, this is more dependant on the burning conditions and the species of wood under test. Once released, the volatiles then react with oxygen in the air and combust in the presence of a suitable ignition source, leading to the formation of carbon dioxide and carbon monoxide. Since these are exothermic reactions, the

heat released sustains the pyrolysis of the wood and char. As more wood is pyrolyzed, the cycle continues until all the wood has been converted to char and all volatiles in the wood have been released.

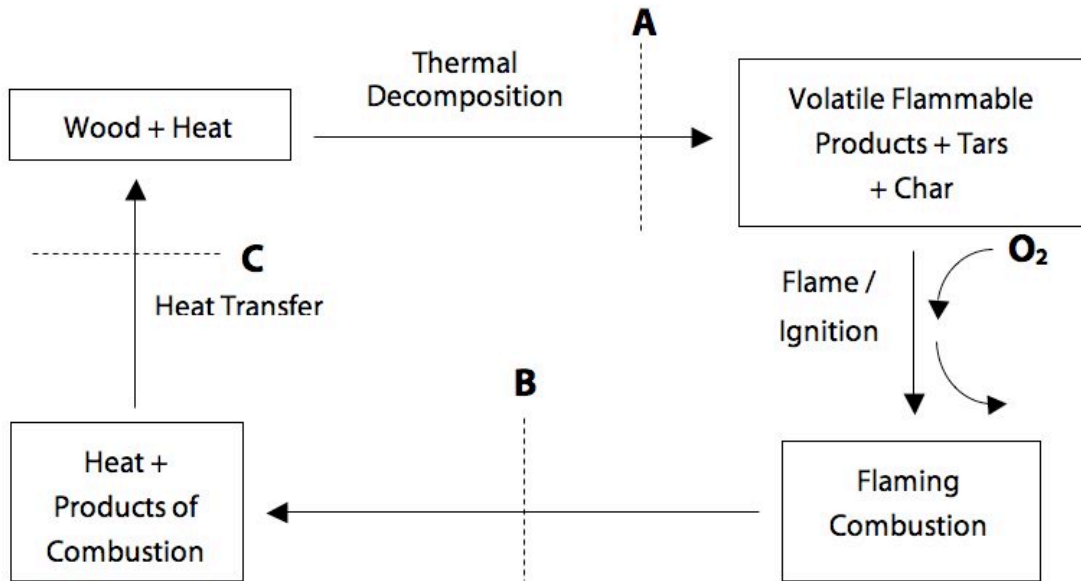


**Figure 3: The Burning Cycle of Wood**

The different polymeric components of wood degrade in different manners. For example, cellulose decomposes between the 260 – 350°C range, and is the reaction that is mainly responsible for the formation of flammable, volatile compounds (Shafizadeh 1984). As the temperature rises and the material degrades, the molecular weight of cellulose decreases (Rowell 1984, Shafizadeh 1984, and LeVan 1990). Since hemicellulose is less thermally stable than cellulose, it degrades in the range of 200 – 260°C. In the process, it also evolves more non-combustible gases and less tar than cellulose (LeVan, et al 1990). Lignin is the most thermally stable component found in wood, and generally pyrolyzes at a slower rate than cellulose or hemicellulose. However, its degradation period commences earlier at around

160°C, and continues degrading until around 400°C. Lignin contributes more to char formation than cellulose or hemicellulose. Increased char formation reduces the emission of flammable gases and helps insulate wood from further thermal degradation (Rowell 1984).

Since the combustion of wood is mainly a function of temperature, the individual phenomena that comprise the process can be followed with rising temperature, as the following table from White and Dietenberger (2002), Babrauskas (2001), Fang (1966), Shafizadeh (1984), LeVan (1990), and Kozlowski (2001) illustrates.

**Table 1: Breakdown of the combustion of wood**

Temperature (°C)	Description
100-200	The wood steadily loses weight and evolves non-combustible gases, such as carbon dioxide, traces of formic, acetic acids and water vapor, through slow pyrolysis.
160	Lignin begins to decompose, resulting in char formation
200 - 260	Exothermic reactions begin, and are characterized by the release of an increased quantity of decomposition gases, as well as the high boiling release point of tar. There is also the appearance of local ignition areas of hydrocarbons with low boiling points.
275 - 280	Uncontrolled release of large amounts of heat occurs and there is an increased production of liquid and gaseous products including methanol, ethanoic acid, and its homologues.
> 280	Beyond 280°C the release of gases increases, and this is accompanied by the rapid formation of charcoal. The

	reactions are highly exothermic when peak temperatures are in the range of 280 – 320°C.
> 300	At this point, if there is sufficient oxygen, the mixture of gases formed will ignite. Combustion proceeds in the gas phase at a small distance from the surface rather than on the wood surface itself. From this moment, wood can burn even after the removal of the heat stimulus. The ignition of wood occurs between 300 – 400°C, depending on the origin of the wood, and will continue to burn until all wood components end their volatile emissions at around 450°C.
> 450	The remaining wood residue is char, which undergoes further degradation by being oxidized to carbon dioxide, carbon monoxide, and water.

## **2.2 An Overview of Fire Retardants**

### **2.2.1 Fire Retardant Mechanisms**

Fire retardants are intended to inhibit and suppress the combustion process through a number of mechanisms and sub-mechanisms. Fire retardants can act chemically and/or physically in the solid, liquid, or gas phase depending on their nature, to retard the combustion process (Troitzsch 1998). They impede a particular stage of the combustion cycle (shown in Figure 3), by modifying the thermal degradation process (A), quenching the flame (B), or reducing the supply of heat from the flame back to the decomposing polymer (C).

### **2.2.2 Physical Processes**

The use of fire retardants gives rise to several physical processes. Firstly, cooling takes place, where endothermic processes triggered by additives cool the substrate to a temperature below that required for sustaining the combustion process.

Secondly, a protective layer (or coating) is formed. The condensed combustible layer can be shielded from the gaseous phase with a solid or gaseous protective layer. The condensed phase is thus cooled and smaller quantities of pyrolysis gases are evolved. The oxygen necessary for the combustion process is excluded and heat transfer is impeded.

Finally, dilution occurs. This is where the incorporation of inert substances (e.g. fillers) and additives that evolve inert gases upon decomposition dilute the fuel in the solid and gaseous phases so that the lower ignition limit of the gas mixture is not exceeded.

### **2.2.3 Chemical Processes**

The most significant chemical reactions interfering with the combustion process take place in the solid and gas phases.

In the gas phase, the free radical mechanism of the combustion process is interrupted by the fire retardant. As a result, the exothermic processes are stopped and the system cools down. The supply of flammable gases is reduced and eventually completely suppressed. Such behavior is often exhibited by halogenated fire retardants.

In the solid phase, the fire retardant can cause a layer of carbon to form on the polymer surface. This occurs, for example through the dehydrating action of the

fire retardant generating double bonds in the polymer. These form the carbonaceous layer by cyclising and cross-linking.

#### **2.2.4 Types of Fire Retardants**

Distinctions are often made between reactive and additive fire retardants. A combination of fire retardants may produce synergistic effects, which are of considerable practical importance since they allow the loading of one or more of the retardants to be reduced without compromising performance. These types are defined below and specific examples are outline in Table 2 (Troitzsch 2004).

Reactive fire retardants are chemically bound to the material, usually via a covalent bond. This prevents the fire retardant from leaching out of the material or volatilizing, thus retaining the material's flame retardance.

Additive fire retardants are incorporated into the material by addition, and are not covalently linked to the substrate. Weaker, secondary bonding interactions such as hydrogen bonding or dipole-dipole interactions may contribute to the retention of the additive in the substrate. This functions much the same way as some preservatives are retained in the wood matrix.

Combinations of additive and reactive fire retardants can produce an additive, synergistic, or antagonistic effect. While the additive effect is the sum of the individual actions, the effects of synergism and antagonism are higher and lower, respectively, relative to the sum. When used alone, synergies show no or only negligible effectiveness. The synergistic effect occurs when they are used together with specific fire retardants. The fire retardant/synergist systems have achieved great importance in practical use because they are usually less expensive than fire retardants used alone.

**Table 2: Examples of additive and reactive fire retardants, which have been used for wood**

Additive Fire Retardants	Reactive Fire Retardants
Simple salts such as mono- and diammonium phosphate, ammonium polyphosphate, ammonium fluoroborate, and ammonium chloride	Chlorendic anhydride (1, 4, 5, 6, 7, 7-hexachloro-5-norbornene-2,3-dicarboxylic anhydride)
Hydrated alumina, magnesium hydroxide	Tetrabromophthalic anhydride
Amino resins. Compounds used for their manufacture are dicyandiamide, phosphoric acid, formaldehyde, melamine, and urea.	Derivatives of polyhydric alcohols such as halogeno-phosphorous polyols, chlorinated bisphenols, and chlorinated neopentyl glycols
Inorganic compounds such as antimony oxide and halogenated hydrocarbons	SF <sub>3</sub> Br
Zinc chloride and boron compounds such as boric acid, sodium tetraborate, zinc borate, triammonium borate, ethyl, and methyl borates	Various halogenated methanes and ethanes, e.g. CH <sub>2</sub> BrCl, CF <sub>2</sub> BrCl, CF <sub>2</sub> Br <sub>2</sub> , CF <sub>2</sub> Br-CF <sub>2</sub> Br

## 2.2.5 Chemical Classes of Fire Retardants

Since the fire retardant under investigation, Burn-X, contains mainly chloride anions and calcium cations, a closer look at fire retardants that contain halogens and inorganic substances is presented.

### 2.2.5.1 Halogen-containing fire retardants

Halogen-containing fire retardants function by trapping free radical species formed during combustion of materials, thereby limiting the propagation of flames (Alaee, et al 2003). The relative effectiveness of the various halogens as flame inhibitors

appear to be directly proportional to their atomic weights (Larson 1974). The effectiveness of halogen-containing fire retardants follow the following order:  $F < Cl < Br < I$ .

Of the four halogens, chlorine and bromine are the most extensively used. Iodine compounds are not used extensively due to their high cost and also because of the high sensitivity of the carbon-iodine bond to thermal and photochemical degradation. Bromine compounds, especially aliphatics, also suffer from poor light stability and high cost. While lowest in cost and highest in light stability (apart from fluorine which is excluded because of its high cost), chlorine compounds are not as effective on a weight basis as the corresponding bromine compounds. Carbon-fluorine bonds are thermodynamically stable up to relatively high temperatures, whereas carbon-iodine bonds disassociate at relatively low temperatures. Bromine is most effective since its bonding to carbon enables it to interfere at a more favorable point in the combustion process. Moreover, it is assumed that the effective agent HBr, is liberated over a narrow temperature range so that it is available at a high concentration in the flame zone. The disadvantage of bromine may often be the relative instability of the carbon-bromine bond as it is subject to thermolysis during processing and photolysis during commercial usage (Kuryla, et al 1978). Chlorine-containing fire retardants release HCl over a wider temperature range. Thus, the latter is considered to be present at relatively lower concentrations, and therefore, less effective.

Both aliphatic and aromatic brominated compounds are used in large quantities as commercial fire retardants. The more effective aliphatic halogen compounds are easier to break down, and hence, are less temperature resistant than aromatic fire retardants. Their suitability depends on the material and the method of incorporation. There is however, increasing concern over the usage of certain brominated fire retardants, since these compounds have been shown to persist in

the environment, bioaccumulate, and may impact human health (Rahman, et al 2002). It is acknowledged that a risk assessment is difficult given the limited knowledge on bioavailability, toxicity, and environmental behavior (de Wit 2002), and there is considerable debate over the toxicity of these compounds.

#### ***2.2.5.2 Inorganic-based fire retardants***

Unlike organic compounds, inorganic fire retardants do not evaporate under the influence of heat. Instead, they decompose, giving off non-flammable gases like water, carbon dioxide, sulfur dioxide, hydrogen chloride, etc, via endothermic reactions.

In the gas phase, these act by diluting the mixture of flammable gases and by shielding the surface of the substrate against oxygen attack. Inorganic fire retardants acts simultaneously on the surface of the solid phase by cooling the substrate via endothermic breakdown process and reducing the formation of pyrolysis products. In addition, as in the case of inorganic boron compounds, a glassy protective layer can form on the substrate, fending off the effects of oxygen and heat.

### ***2.3 Equipment***

#### **2.3.1 Cone Calorimeter**

The cone calorimeter is an instrument that can be used to burn small samples of various materials to gather data about combustion products, heat release, and other such products associated with combustion.

This fire-testing instrument is based on the principle of oxygen consumption calorimetry, according to WPI's Department of Fire Safety. This empirical principle is based on the observation that generally, the net heat of combustion of any organic material is directly related to the amount of oxygen required for combustion. For each kilogram of oxygen consumed, approximately 13.1 MJ of heat is released during combustion for most solids (Redfern 1989).

At the core of the instrument lies a radiant electrical heater, in the shape of a truncated cone. This heating element can irradiate a flat, horizontal sample placed beneath it at a preset heat flux. To continuously monitor the mass of the sample as it burns, the test piece is placed on a load cell. An intermittent spark igniter located above the sample provides ignition. Figure 4 (WPI Dept of Fire Protection Engineering – Cone Calorimeter, 2006) shows a typical setup of a cone calorimeter.

The gas stream containing the combined combustion products is captured through an exhaust duct system, which consists of a high-temperature centrifugal fan, a hood, and an orifice-plate flowmeter. Oxygen concentration in the exhaust stream is measured with an oxygen analyzer capable of achieving accuracy of up to 50 ppm. The heat release rate is determined by comparing the oxygen concentration with the value obtained when no sample is burning.

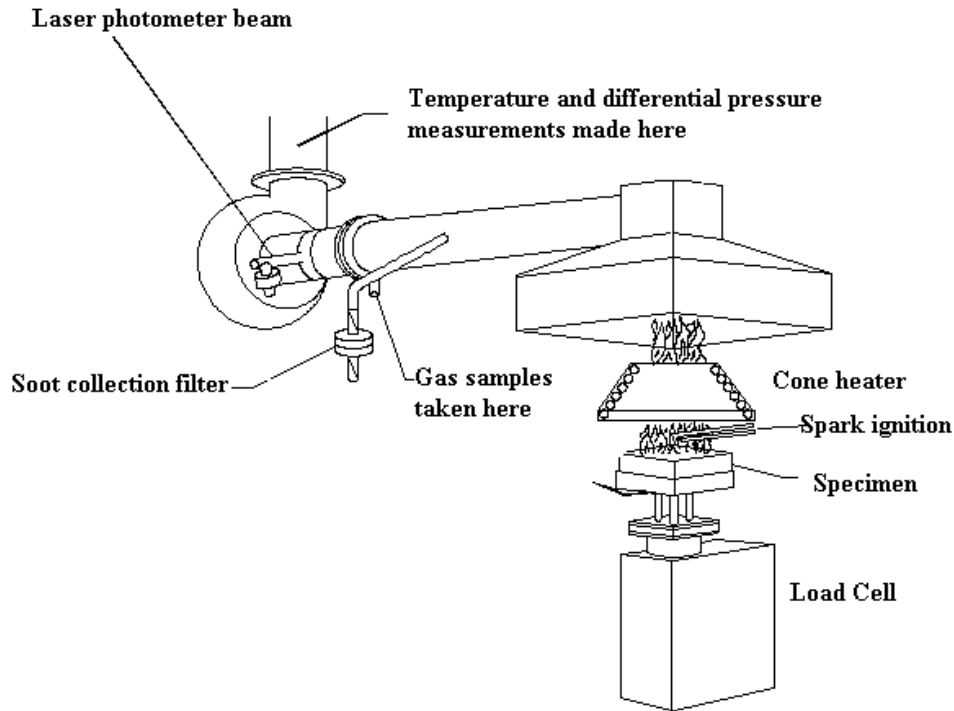


**Figure 4: Typical cone calorimeter setup**

In addition, smoke obscuration measurements are made in the exhaust duct by a helium-neon laser, with silicon photodiodes as main beam and reference detectors, and appropriate electronics to derive the extinction coefficient and set the zero reading. Locations are also provided in the exhaust duct for addition sampling probes, to determine concentrations of other combustion products, such as the carbon oxides.

The CSIRO cone calorimeter, however, is not like all other commercially available cones. Several modifications were made to it over the past few years. Firstly, the CSIRO cone calorimeter uses liquid nitrogen cooling. Not only was it found to be a more efficient method, but also is much better for the environment.

In addition, the gas analyzer taps have heating elements, so the gases do not condense. Finally, this cone also has the ability to perform CO/CO<sub>2</sub> measurements – a feature that proved to be very useful to this investigation.

The cone calorimeter at CSIRO is set up as illustrated in Figure 5 (figure obtained from Ashley Bicknell, CMIT CSIRO).

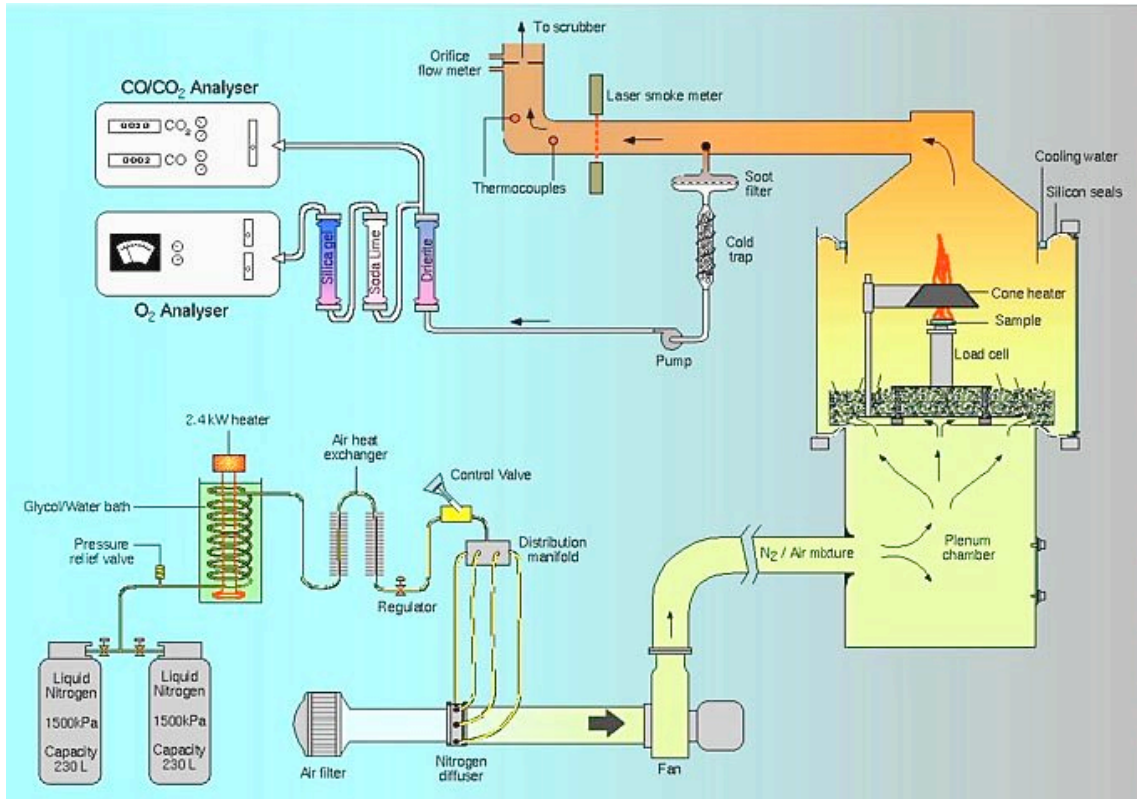


**Figure 5: CSIRO cone calorimeter schematic**

All data were collected with a PC, which continuously recorded data at fixed intervals of a few seconds while a test was being conducted.

The cone calorimeter at CSIRO (pictured in Figure 6) can be used to determine the following principal fire properties:

- rate of heat release per unit area;
- cumulative heat released;
- effective heat of combustion;
- time to ignition;
- mass loss rate;
- total mass loss; and
- smoke obscuration.



**Figure 6: Cone calorimeter at CSIRO**

The test method used with the cone calorimeter was the ASTM E 1354, which even though is only about ten years old, appears to be the best possibility for a single, comprehensive test that satisfies most usage sectors.

Several advantages of this test are that the sample size is modest, keeping preparation costs low, testing costs are also usually modest (they range from \$200-\$500 in most commercial labs), and most of the fundamental combustion characteristics can all be determined under a wide range of heater and ignition conditions. As a result of the vast amount of data available from this test, a model of the combustion of a material can be developed, thus enabling estimation of the potential effects of fire on surrounding areas and occupants.

### **2.3.2 TGA-DTGA / DTA<sup>1</sup>**

TGA, or thermogravimetric analysis, measures the weight loss of the material as a function of temperature. It is a great tool for the qualitative and quantitative analysis of a sample as it is heated. Physical changes in the sample that do not involve a change in energy, such as a phase change, are captured in the DTA curve, making this an important and powerful tool in solid state chemistry and materials science. For example, the method can be used to determine water of crystallization, follow the degradation of materials, determine reaction kinetics, study oxidation and reduction, or to teach the principles of stoichiometry, formulae, and analysis. The TGA curve also provides information concerning the thermal stability of the initial sample, initial compounds that may be formed, or the formation of residue. In the case of weight loss in a sample, the TGA can quantify and predict the pathway of degradation or obtain compositional information (Sharatov 2001).!

---

<sup>1</sup> Thermogravimetric Analysis (TGA) – Differential Thermogravimetric Analysis (DTGA) / Differential Thermal Analysis (DTA)

Very often, thermal changes such as phase transitions in materials do not involve a change in mass. Therefore, in the DTA, we can instead measure the temperature difference between an inert reference and the sample as a function of temperature. While undergoing a physical or chemical change, the temperature increase between the material and the inert reference differs, and a dip or peak is detected in the DTA signal (Dolmer 2006).

This technique can be applied to a wide range of studies, such as:

- identification;
- quantitative composition analysis;
- phase diagrams;
- hydration-dehydration;
- thermal stability;
- polymerization;
- purity; and
- reactivity.



**Figure 7: External View of the TGA-DSC**

A TA Instruments Q600 Simultaneous Thermogravimetric Analyzer – Differential Scanning Calorimeter (TGA-DSC) is used at CSIRO's facility, and is pictured in Figure 7. This instrument provides a true simultaneous measurement of weight change (TGA) and heat flow (DSC) on the same sample from ambient to 1 500°C as a function of temperature or time. It also has the ability to analyze two TGA samples simultaneously. The following figure shows an internal view of the apparatus and the two pans, in which the samples are placed.

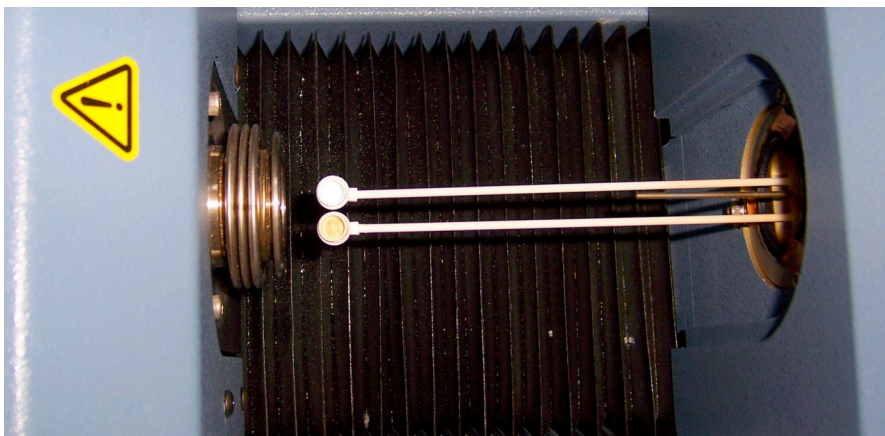


**Figure 8: Sample holders in the TGA-DSC apparatus**

### 2.3.3 FTIR

FTIR, or Fourier-Transform Infrared Spectroscopy is a chemical analytical technique that measures infrared intensity versus the wavenumber or wavelength of light. Infrared spectroscopy detects the vibrational characteristics of chemical functional groups in a sample. When IR light interacts with matter, chemical bonds contract, stretch, or bend. Therefore, chemical functional groups tend to adsorb IR radiation in a specific wavenumber range regardless of the structure of the rest of the molecule, according to KISS NUANCE center at Northwestern University.

They further give the example that a C=O stretch of a carbonyl group appears at around  $1700\text{ cm}^{-1}$  in a variety of molecules. Hence the correlation of the band wavenumber position with the chemical structure is used to identify a functional group in a sample. The wavenumber positions where functional groups adsorb are consistent, despite the effect of temperature, pressure, sampling, or change in the molecule structure in other parts of the molecules. Thus these types of infrared bands, which are called group wavenumbers, can monitor the presence of specific functional groups.

An FTIR spectrometer obtains data by collecting an interferogram, which simultaneously measures all the IR frequencies. According to Chen (2006) at the Keck-II center in Northwestern University, "an interferometer utilizes a beamsplitter to split the incoming infrared beam into two optical beams. One beam reflects off of a flat mirror which is fixed in place. Another beam reflects off of a flat mirror which travels a very short distance (typically a few millimeters) away from the beamsplitter. The two beams reflect off of their respective mirrors and are recombined when they meet together at the beamsplitter. The re-combined signal results from the "interfering" with each other. Consequently, the resulting signal is called interferogram, which has every infrared frequency "encoded" into it. When the interferogram signal is transmitted through or reflected off of the sample

surface, the specific frequencies of energy are adsorbed by the sample due to the excited vibration of function groups in molecules. The infrared signal after interaction with the sample is uniquely characteristic of the sample. The beam finally arrives at the detector and is measure by the detector. The detected interferogram cannot be directly interpreted. It has to be "decoded" with a well-known mathematical technique in term of Fourier Transformation. The computer can perform the Fourier transformation calculation and present an infrared spectrum, which plots adsorbance (or transmittance) versus wavenumber.

When an interferogram is Fourier transformed, a single beam spectrum is generated. A single beam spectrum is a plot of raw detector response versus wavenumber. A single beam spectrum obtained without a sample is called a background spectrum, which is induced by the instrument and the environments. Characteristic bands around  $3\ 500\ \text{cm}^{-1}$  and  $1\ 630\ \text{cm}^{-1}$  are ascribed to atmospheric water vapor, and the bands at  $2\ 350\ \text{cm}^{-1}$  and  $667\ \text{cm}^{-1}$  are attributed to carbon dioxide. A background spectrum must always be run when analyzing samples by FTIR. When an interferogram is measured with a sample and Fourier transformed, a sample single beam spectrum is obtained. It looks similar to the background spectrum except that the sample peaks are superimposed upon the instrumental and atmospheric contributions to the spectrum. To eliminate these contributions, the sample single beam spectrum must be normalized against the background spectrum.

The final transmittance/absorbance spectrum should be devoid of all instrumental and environmental contributions, and only present the features of the sample. If the concentrations of gases such as water vapor and carbon dioxide in the instrument are the same when the background and sample spectra are obtained, their contributions to the spectrum will ratio out exactly and their bands will not

occur. If the concentrations of these gases are different when the background and sample spectra are obtained, their bands will appear in the sample spectrum.”

Figure 9 shows the Nexus GC-FTIR equipment used in the CSIRO laboratories.



**Figure 9: FTIR Apparatus**

An output from the DSC-TGA apparatus was used as the sample feed for the FTIR, as can be seen in Figure 10 so that gases emitted during the combustion and pyrolysis reactions could be monitored.



**Figure 10: FTIR and TGA-DSC equipment being used in conjunction**

### **2.3.4 Porosimeter**

A Quantachrome Autosorb-1 porosimeter is used at the CSIRO facilities. To gain a better understanding of the apparatus, an extract from the company brochure was taken.

“In gases, atoms and molecules are free to move about in space. In contrast, atoms in solids are located in fixed positions by electrical forces of attraction among neighboring atoms. But the outermost (or surface) atoms in the solid have fewer neighbors than the atoms beneath them in the bulk. To compensate for their electrical force imbalance, surface atoms seek to attract surrounding gas molecules. The tendency of all solid surfaces to attract surrounding gas molecules gives rise to a process called gas sorption. Monitoring the gas sorption process provides a wealth of useful information about the characteristics of solids.

Before performing gas sorption experiments, solid surfaces must be freed from contaminants such as water and oils. Once clean, the sample is brought to a constant temperature by means of an external bath. Then, small amounts of a gas (the adsorbate) are admitted in steps into the evacuated sample chamber.

Adsorbate molecules quickly find their way to the surface of every pore in the solid (the adsorbent). These molecules can either bounce off or stick to the surface. Gas molecules that stick to the surface are said to be adsorbed. The strength with which adsorbed molecules interact with the surface determines if the adsorption process is to be considered physical (weak) or chemical (strong) in nature.

Physical adsorption (physisorption) is the most common type of adsorption. Physisorbed molecules are fairly free to move around the surface of the sample. As more gas molecules are introduced into the system, the adsorbate molecules tend to form a thin layer that covers the entire adsorbent surface. Based on the well known Brunauer, Emmett and Teller (BET) theory, one can estimate the number of molecules required to cover the adsorbent surface with a monolayer of adsorbed molecules.

Continued addition of gas molecules beyond monolayer formation leads to the gradual stacking of multiple layers (or multilayers) on top of each other. The formation of multilayers occurs in parallel to capillary condensation. The latter process is adequately described by the Kelvin equation, which quantifies the proportionality between residual (or equilibrium) gas pressure and the size of capillaries capable of condensing gas within them. Computational methods such as the one by Barrett, Joyner, and Halenda (BJH) allow the computation of pore sizes from equilibrium gas pressures. One can therefore generate experimental curves (or isotherms) linking adsorbed gas volumes with relative saturation pressures at equilibrium, and convert them to cumulative or differential pore size distributions.

As the equilibrium adsorbate pressures approach saturation, the pores become completely filled with adsorbate. Knowing the density of the adsorbate, one can calculate the volume it occupies and, consequently, the total pore volume of the sample. If at this stage one reverses the adsorption process by withdrawing known

amounts of gas from the system in steps, one can also generate desorption isotherms. Since adsorption and desorption mechanisms differ, adsorption and desorption isotherms rarely overlay each other. The resulting hysteresis leads to isotherm shapes that can be mechanistically related to those expected from particular pore shapes.

In contrast to physisorption, chemical adsorption (chemisorption) involves the formation of strong chemical bonds between adsorbate molecules and specific surface locations known as chemically active sites. Chemisorption is thus used primarily to count the number of surface active sites that are likely to promote chemical and catalytic reactions.

The functions of the porosimeter are diagrammed in Figure 11, and can perform the following:

- surface area measurements;
- adsorption/desorption isotherms;
- pore size distributions;
- chemisorption studies;
- true solid density; and
- water vapor sorption.



**Figure 11: Quantachrome Porosimeter**

## **2.4 Data collection Parameters**

Using the aforementioned equipment, large amount of data on the combustion of wood was collected. The cone calorimeter was used for burn analyses and a HRR curve was produced. The volumetric sorption analyzer was to be used for surface area and pore size measurements of the char, and the TGA-DTA was used for proximate analyses of chars, such as moisture, volatile matter, and ash.

### 2.4.1 Heat Release Rate (HRR)

Once ignited, wood undergoes flaming combustion and releases heat. The HRR is a measure of the energy released per unit time per unit area exposed [ $\text{kW m}^{-2}$ ]. An HRR curve is the primary result obtained from a cone calorimeter test. The HRR due to combustion is determined using the oxygen consumption methodology, which is derived from the observation that the net heat of combustion is directly related to the amount of oxygen required for combustion. It may also be important to note that the method does not account for the condensation of water produced from burning the fuel.

A general pattern is found in all HRR curves for wood. Following ignition, a peak HRR occurs, which is a result of burning the combustible pyrolysate soon after ignition. As the wood chars, somewhat of an exponential decay follows, because of the insulating effect of the char layer. It is believed that the char, which is relatively stable, traps volatile matter within the material. If the wood sample is sufficiently thick, the HRR will stabilize to a steady rate. However, for materials with finite thickness, a second peak occurs near the end of the burning, as the bulk temperature of the remaining material is rapidly raised to a higher value. The collapsing char leads to the release of volatile matter, and thus, the second decay occurs. An example of a generic HRR curve for untreated pine (specie *Pinus Radiata*) is shown in Figure 12.

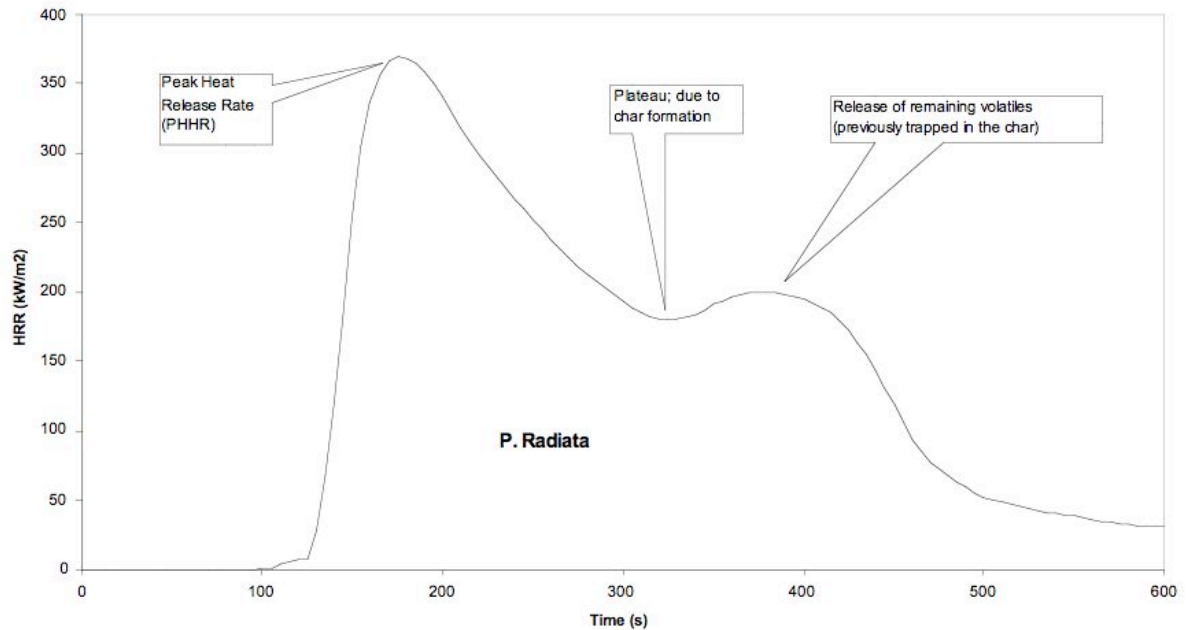


**Figure 12: Heat Release Rate curve for untreated timber at 25 kW m<sup>-2</sup>**

Generally, the part of the HRR curve that is of most interest in modeling fire growth is the second peak, which is dependent on unexposed face conditions.

The HRR curve is often reduced to single numbers for reporting purposes, namely the initial PHRR and the averages of the HRR over set times (for example 60, 180, and 300 seconds) after ignition of the specimens. The problem with the peak HRR is that its single value that can be missed as a result of the discrete data-sampling interval of many seconds. The error can be large since this peak occurs in steep regions of the curve.

From studies conducted by Tran and White (1992), they have found HRR measurements to be the most useful since they are readily measured in oxygen consumption calorimeters. This also allows the calculation of mass loss and charring rates for wood materials. However, only two parameters need to be known: the effective heat of combustion, and density. Heat of combustion and

mass loss rate data can be measured with advanced calorimeters such as the cone calorimeter. Therefore, HRR or mass loss rate can be used to characterize burning rate and be used to derive the charring rate of wood.

On the other hand, we can also look at HRR curves for fire retardant treated wood. As can be seen in Figure 13, there is significant difference in HRRs between treated and non-treated woods. First, the PHRR for treated wood ( $\sim 200 \text{ kW m}^{-2}$ ) is much lower than that of untreated wood ( $365 \text{ kW m}^{-2}$ ), which can be attributed to the fire-retardant coating. For fire-treated wood, the decrease to the plateau after the PHRR is not as sharp as that for untreated wood. Furthermore, the second peak in untreated wood is also much lower and less pronounced.

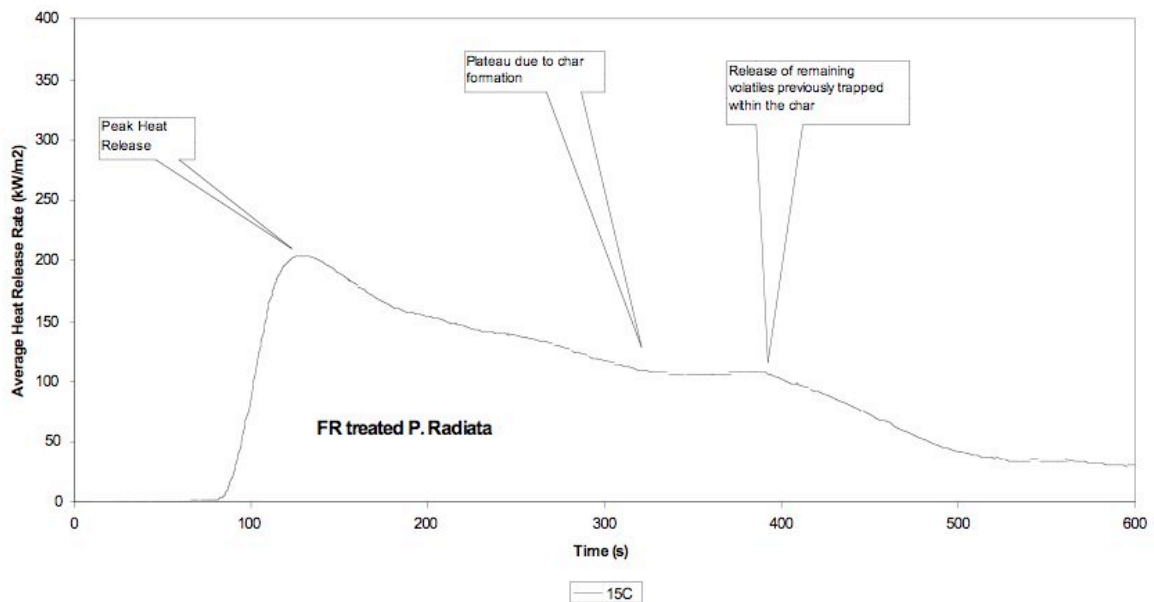


**Figure 13: HRR curve for Burn-X treated wood at  $25 \text{ kW m}^{-2}$  (plot obtained from Dr Donovan Marney, 2006, CMIT, CSIRO)**

## **2.4.2 Thermogravimetric Curves**

Thermogravimetric (TG) curves show the variation of the sample mass with heating temperature or time. From these curves, it is possible to derive information on the amount of char formed at any given temperature or time. After the commencement of decomposition, a higher sample mass at any given temperature or time implies the formation of more char residue.

The derivative thermogravimetry (DTG) curves show the mass loss rate of the sample as a function of temperature or time, and consist of a series of peaks corresponding to the various stages in the decomposition process. The DTG curves may be used to quantify the bulk changes evident in the TG curves, and provide an indication of the thermal stability of a material.

## **2.5 Kinetics**

According to Helsen and van den Bulck (2000), "the use of TGA to determine kinetic parameters for the pyrolysis of wood is complicated in that the decomposition of wood represents a large number of reactions in parallel and series whilst the TGA measures the overall weight loss due to these reactions." An example of parallel reactions can be found in the pyrolysis of wood, where it is commonly believed that three parallel mechanisms govern the degradation. As a result, instead of providing overall reaction kinetics, thermogravimetric analyses only provide individual reactions. In theory, endless varieties with varying degrees of reaction complexities can be assumed in wood pyrolysis, but it is the aim of kinetic evaluation of TG data to obtain relatively simple models that can be utilized to form a complete theoretical model that effectively describes the mechanisms that occur within the wood.

## **2.5.1 Kinetic Parameters**

A brief explanation of the kinetic parameters is presented below to gain insight on the elements that make up the Arrhenius rate law, which is “a simple, but remarkably accurate, formula for the temperature dependence of a chemical reaction rate, more correctly, of a rate coefficient, as this coefficient includes all magnitudes that affect reaction rate except for concentration” according to the IUPAC Goldbook.

### ***2.5.1.1 Pre-exponential Factor***

Usually designated by the letter  $A$ , the pre-exponential factor is the empirical relationship between the temperature and rate constant. It can also be referred to as the collision frequency factor, since it represents the frequency collisions occur at.

### ***2.5.1.2 Rate constant***

Designated by  $k$ , the rate constant quantifies the speed of a chemical reaction. It includes all the factors that may affect the rate of reaction (except concentration).

### ***2.5.1.3 Activation Energy***

Activation energy, or  $E_a$ , is the minimum energy that must be overcome in order for a chemical reaction to occur. This is a useful parameter since it can give an idea of the energy required for a whole reaction to proceed. Activation energies also aid in gaining further insight to the mechanistic nature of any given reaction.

## **2.5.2 The Broido Model**

The kinetics of both pyrolysis and combustion can often be described by first order Arrhenius laws (Rath and Staudinger 2001). We can assume that each of the processes

of pyrolysis and combustion can be divided into two steps (low and high temperatures) and each are governed by first order Arrhenius law (Shi 2004). Broido (1969) developed a model to specifically deal with the thermal analysis of cellulosic substances. This model was used in this investigation to evaluate the kinetic parameters necessary. The following is a brief derivation.

The mass loss fraction can be defined as

$$y = \frac{N}{N_0} = \frac{W_t - W_\infty}{W_0 - W_\infty} \quad (1)$$

Since the pyrolysis is carried out isothermally, the reaction rate can be defined by

$$\frac{dy}{dt} = -ky^n, \text{ where } n \text{ is the reaction order} \quad (2)$$

If the rate constant,  $k$ , changes with absolute temperature according to the Arrhenius equation:

$$k = Ae^{-\frac{E}{RT}} \quad (3)$$

Equations (2) and (3) can be combined to give

$$\frac{dy}{y^n} = -Ae^{-\frac{E}{RT}} dT \quad (4)$$

The TGA curve for such a reaction represents equation (3) integrated from a temperature  $T_0$  at which  $y=1$ . Thus,

$$\int_y^1 \frac{dy}{y^n} = A \int_{T_0}^T e^{-\frac{E}{RT}} dT \quad (5)$$

But since a large number of pyrolysis processes can be represented as first-order reactions, we can consider mainly such reactions. Therefore,

$$\int_y^1 \frac{dy}{y^n} = \int_y^1 \frac{dy}{y} = -\ln y = \ln(1/y) \quad (6)$$

Upon applying approximation techniques and integrating (see Broido 1969 for more details), we get

$$\ln \left[ \left( \ln \frac{1}{y} \right) \right] = -\frac{E_a}{R} \frac{1}{T} + \text{const.} \quad (7)$$

The constant is evaluated by Gao (2004), resulting in

$$\ln \left[ \left( \ln \frac{1}{y} \right) \right] = -\frac{E_a}{R} \frac{1}{T} + \ln \left( \frac{R}{E_a} \frac{Z}{\hat{a}} T_m^2 \right) \quad (8)$$

In equation (8),  $y$  represents the fraction of initial molecules not yet decomposed,  $T_m$  is the temperature of maximum reaction rate,  $\beta$  is the rate of heating,  $Z$  the frequency factor, and  $E_a$  is the activation energy.

Since the term  $\ln[\ln(1/y)]$  varies linearly with  $(E_a/RT)$ , plots of  $\ln[\ln(1/y)]$  vs  $1/T$  were made. The activation energies were determined from the slope of the linear plots obtained.

## **3 Methodology**

### **3.1 Sample Preparation**

Two sets of specimens were necessary to carry out this investigation: a set of untreated timber that was used as a control, and the fire retardant treated timber. Both the sample specimen sets were treated using the vacuum impregnation process, using water as a solvent, and a Burn-X solution respectively.

The fire retardant treatment solutions were prepared by diluting the respective concentrate to the appropriate concentration, based on an average uptake of solvent (water; 1.54 g g<sup>-1</sup> oven dry wood; white spirit alcohol 1.11 g g<sup>-1</sup> oven dry wood).

The timber specimens, measuring 50 mm x 50 mm x 10 mm (longitudinal x tangential x radial), were treated to Hazard Class 3 retentions, as stated in AS 1604.1 – 2000. The specimens were weighted down in a vacuum desiccator and a vacuum of -90 kPa was applied for thirty minutes. The treatment solution was admitted to the desiccator under vacuum, after which the vacuum was released and the specimens left to adsorb solution at atmospheric pressure for sixty minutes. Each specimen was weighed before and after treatment to determine the uptake. After treatment, the specimens (except solvent controls) were wrapped in plastic bags and left for one week, then slowly air-dried. The specimens were then vacuum oven dried at -90 kPa and 40°C for five days, after which they were reconditioned to an estimated moisture content of approximately 10%. The vacuum pressure method is outlined and diagrammed as follows in Figure 14 from the *How to Use Burn-X* guide, which was provided by the manufacturers of the chemical.

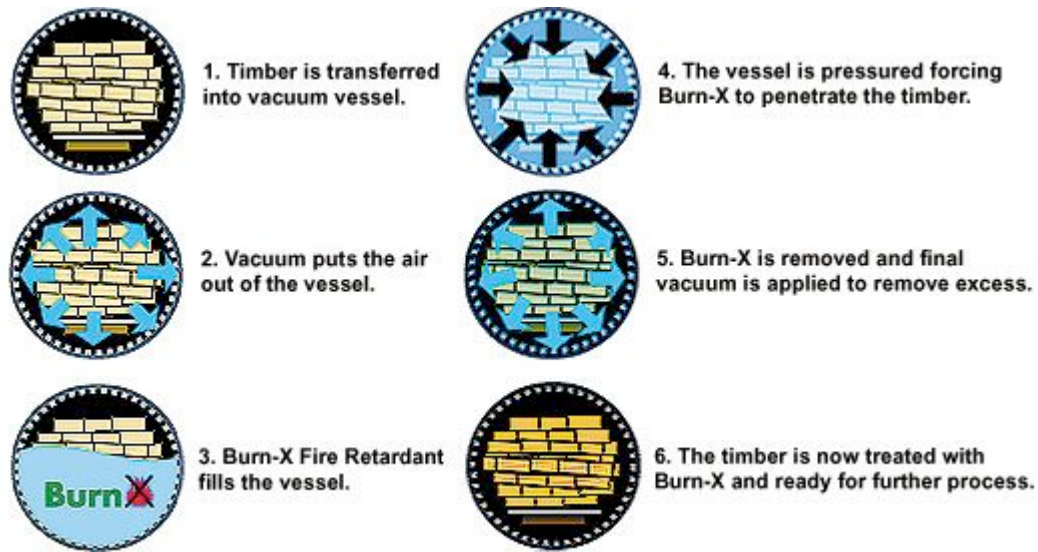


Figure 14: Vacuum Pressure Method

## 3.2 Cone Calorimetry Pilot Tests

### 3.2.1 Determining the Heat flux

Before proceeding to use the cone calorimeter, it was important to establish which irradiance level was the most appropriate for the samples. In order to establish this, two sets of samples were tested, both of which consisted of untreated wood. Three samples were tested at  $25 \text{ kW m}^{-2}$  and another three at  $35 \text{ kW m}^{-2}$ . Standard cone calorimeter procedure was used for testing, which is detailed in Appendix B.

One of the first things we wanted to check is the reproducibility of results at the different heat fluxes, to ensure that the irradiance does not affect the results in any way. Secondly, we wished to establish which heat flux gave results that would be more suitable to use in further data analysis.

Two sets of data were obtained from the cone calorimeter, which included the *HRR curve*, *E Heat of Combustion*, *CO* and *CO<sub>2</sub>* gas release rate, *Specific Area of Extinction*,

Mass loss, Mass Loss Rate, as well as the Average Mass Loss over 1 minute. Of these, the Heat Release Rate curves were used the most in the selection of the heat flux.

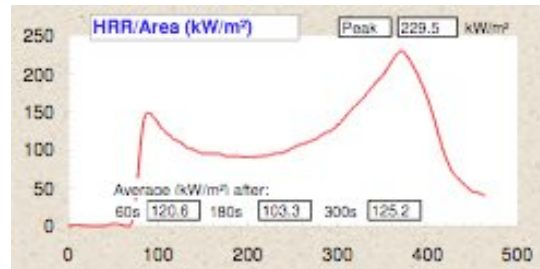


**Figure 15: HRR for 25 kW m<sup>-2</sup> sample**

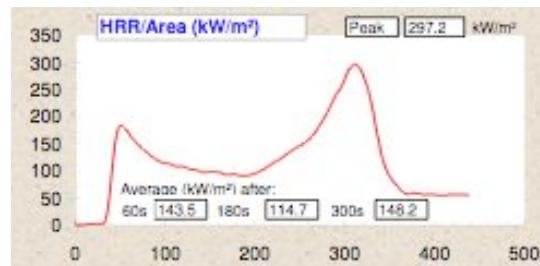


**Figure 16: HRR for 35 kW m<sup>-2</sup> sample**

Comparing the two sets of HRR curves, it was quite clear that the heat flux did not affect the development of the combustion process, since both the curves seem to have the same shape and trends. It also appears that the peaks in the 25 kW m<sup>-2</sup> data are sharper and easier to isolate, as can also be seen in Figure 15 and Figure 16. Due to the higher irradiance, the HRR curves for the 35 kW m<sup>-2</sup> tests occur over a shorter period of time, consequently making the data seem more 'compressed'. Likewise, the troughs of the HRR curves in the 25 kW m<sup>-2</sup> irradiances tests are also easier to isolate since there is extra time compared to the other set, increasing the available resolution.

During the selection process, it was argued that the 35 kW m<sup>-2</sup> heat flux tests would take less time, and increase productivity, since they are almost 100 seconds shorter than the 25 kW m<sup>-2</sup> heat flux tests. However, it was concluded that this was not a

significant length of time compared to the fact that the  $25 \text{ kW m}^{-2}$  data was clearer to read. Another advantage to using the  $25 \text{ kW m}^{-2}$  heat flux is that it is a commonly used benchmark in the industry, and would help make the data more comparable with a wider range of data.

### **3.2.2 Determining Key Times**

In order to gain full understanding of the burning processes, the samples were quenched at different time intervals, and then further analyzed using a porosimeter. However, it was important to select intervals that would be critical points in the burning process, and would contain the maximum amount of information for the subsequent tests.

Referring to Figure 15 it is clear that there are three critical points on the HRR curve for untreated timber: the two peaks and the trough between them. Figure 13 shows a HRR curve for timber treated with the fire-retardant, it can be seen that the two peaks would be our points of interest.

To determine the time when these points occur, HRR curves for three samples of fire-retardant treated and three samples of untreated timber were obtained by burning each of them in the cone calorimeter, using the heat flux determined from the previous section. The total of the four time intervals obtained were to be used as quenching and analysis points for all the samples—treated and untreated, in combustion and pyrolysis conditions.

### **3.2.3 Pilot Test Discussion**

Cone testing was carried out as outlined over the period of a week. However, it was found that the test results lacked consistency. After discussing and analyzing the results and methodology at length, we realized there was an error in the methodology implemented. The main problem was that the treated and untreated pine samples we received from ENSIS were conditioned to have very little moisture content. However, upon receiving them, we placed them in our conditioning cabinet, which was at 23°C and 50% relative humidity— conditions that were extremely different to those they were produced at. This resulted in the samples gaining moisture over time, which in turn affected their behavior; characteristics such as ignition temperature, time to ignition, and heat released changed drastically with the moisture content.

Without a relatively consistent set of results, we decided it would be useless to proceed without changing the methodology, since the times that the samples were quenched at would no longer be representing the same snapshot period of the reaction. It was proposed that the timber specimens be drained of all the moisture content, but that would have taken a long period of time, and even then one could not be sure that all the specimens were identical. As a result, we decided it would be better if all the samples were conditioned at 23°C and 50% r.h. for a week. Over the period of a week, the masses were monitored for changes, and it was found that for the treated samples an average mass increase of over 23% was noted. The mass change for untreated was not so drastic, as they only gained approximately 3% mass on average. At the end of the conditioning week, minor mass changes in mass were still being noticed. However, given the time limitations, it was no longer possible to wait more for the samples to come into 'perfect equilibrium' with the conditions.

The newly conditioned specimens were tested in the cone to observe what changes occurred in ignition time, HRR, etc. Due to a limitation in the number of specimens available, only two samples of the untreated pine were re-tested, and three samples of the treated pine. With the untreated pine, the HRR curve was delayed by approximately twenty seconds. This can be attributed to the higher moisture content, which effectively delayed ignition. The changes with the treated pine were significantly more drastic. Instead of the two peaks that were previously observed, there was now only one peak that occurred much later in the reaction. The flame was also present for a significantly shorter time.

By this stage, all the cone tests for combustion of treated and untreated wood had already been completed, and enough samples to repeat all the tests would not have been available for a period of approximately three more weeks.

Using the newly conditioned treated timber cone data, a quenching time was established from the average peak time. This point was then used to quench the reaction in low oxygen pyrolysis tests of the treated samples.

### ***3.3 Cone Calorimeter testing***

The experimental part of the cone calorimeter testing was divided into two major parts: complete combustion test conditions, and low oxygen pyrolysis conditions. Testing was then further broken down to untreated and treated specimens. Each sample was to be quenched at the four times that were determined from the previous sections. Furthermore, each sample was repeated three times to ensure accuracy of the data.

The following shows the individual breakdown of the tests performed.

- Untreated

- 3 samples x 4 times = 12
- Treated
  - Combustion: full O<sub>2</sub> environment
    - 3 samples x 2 times = 6
  - Pyrolysis: reduced O<sub>2</sub> environment
    - 3 samples x 1 time = 3

### 3.3.1 Liquid Nitrogen Quenching

In order to gain knowledge of the workings of the reactions at different points of the combustion/pyrolysis process, 'snapshots' were taken by quenching the samples. Several techniques were proposed, some of which involved immersion in water, immersion in liquid nitrogen, and immersion in a cold air stream of the sample after being removed from the cone. However, after much discussion we decided to use liquid nitrogen as the coolant.

It was important that there was no direct contact between the coolant and the sample, such as would be the case with complete immersion, since it was possible that the char structure could be affected, and pore sizes altered.



Figure 17: Liquid Nitrogen quenching apparatus

As a result, we developed an apparatus (see Figure 17) in which we could take the sample (still in its holder) out of the cone and place it on a raised area in a sealable container. Liquid nitrogen would then be poured out of a flask until the container was approximately one-third full, as shown in Figure 18.

We believe the rapidly evaporating nitrogen gas was enough to cool the sample fast enough to stop a large part of the reactions taking place in a manner that would not physically damage the specimen.

This was carried out under a fume hood to ensure the safety of those present in the laboratory. The sample was left in the apparatus until all the liquid nitrogen had evaporated.



**Figure 18: Wood sample from cone being cooled**

### 3.3.2 Combustion Method

The following is a detailed method that was followed for cone testing. The pre-test procedure and methanol calibrations were only performed once daily prior to sample testing.

#### 3.3.2.1 Pre-Test Procedure

1. Ensure power is on to CO/CO<sub>2</sub> and O<sub>2</sub> analyzers, as they need 24-hour warm up. Nitrogen should be bled through the O<sub>2</sub> analyzer if it has been turned off for any length of time. The cone generally should *never* be turned off except for some maintenance procedures.
2. Load 'Test Record' software – there is an icon on the computer's desktop. Select 'Enable macros' when prompted.
3. Maximize the 'Misc' (miscellaneous) screen.
4. Check that the Differential Pressure displayed on the screen is zero  $\pm 0.125$  before anything is turned on. Adjust if necessary using the 'Delta P zero' knob.
5. Change soot filter.
6. Replenish all vials as necessary.
  - Drierite is reused (Oven @ 200°C for 1 hour) one layer thick
  - Silica Gel is reused (Oven @ 90°C for 1 hour)
  - Soda Lime is thrown out
7. Press front panel buttons 'laser' and 'cold trap'.
8. Turn water ON (~30 psi).
9. Purge air ON (~10 L/min) at rear of cone. (Starts at ~15 L/min when not running).

10. Scrubber ON (near fume cupboard). Check pump pressure (outside door above hinge) is in the green, if not check scrubber tank is full.
11. Fan ON (front panel).
12. Fan control (front panel) switch to 'loop'. (2 clicks as middle is OFF)
13. Pump ON (front panel). (Check that all flow meters are registering. If not check pump).
14. On CO/CO<sub>2</sub> analyzer, press <O> in and out quickly. This sends the analyzer into a calibration mode (takes ~30 seconds). (▷0◁ symbol appears, then returns to zero).
15. Check that the O<sub>2</sub> analyzer pressure is registering 108.4 Pa on the 'Misc' screen. If not, adjust pressure using the big round knob on the front of the cone. (Undo locking nut if necessary) and by adjusting backpressure valve (small black knob to left of O<sub>2</sub> pressure Regulator).
16. Check that the % O<sub>2</sub> is registering 20.95 on the 'Misc' screen. If not, adjust using the RH red knob inside the O<sub>2</sub> analyzer cabinet.
17. Adjust O<sub>2</sub> analyzer baseline to ~2 L/min (white ball sits on top of mark) using 'B' knob and span to 3.5 L/min using the 'S' knob.
18. Adjust the CO/CO<sub>2</sub> flow meter to ~2 L/min (silver ball sits on top of mark) using the CO/CO<sub>2</sub> flow knob.
19. Pump OFF.
20. Fan OFF and flick fan controller toggle switch to manual.
21. Turn flow control knob to 'zero'. This opens the N<sub>2</sub> gas line to the O<sub>2</sub> analyzer.

22. Turn N<sub>2</sub> on slowly using top valve on wall and adjust flow, to give a supply pressure of 108.4 Pa on the computer screen. It will take ~10 minutes for the system to equilibrate.
23. After the system has equilibrated, adjust % O<sub>2</sub> so computer screen reads 0 ± 0.003 using the LH red zero knob inside the O<sub>2</sub> analyzer cabinet.
24. While the system is equilibrating from 22 above, turn special cal gas on slowly, (lower black knob on wall). Adjust flow to 2 L/min – ball sits on top (using the lower black knob) and allow gas to equilibrate (two or three minutes). Adjust spans on CO/CO<sub>2</sub> analyzer (10 turn pots) using the CO/CO<sub>2</sub> flow knobs, to give a display reading for both gases within the range specified on the calibration card.  
(CO 861 ± 17 and CO<sub>2</sub> 4.09 ± 0.1)
25. Switch off all gases. Wait until there is no pressure before moving flow control valve.
26. Turn flow control to 'sample'. This enables normal sample atmosphere to be drawn into the analyzer.
27. Switch ON fan and switch fan controller to 'loop'.
28. Pump ON.
29. Allow all calibration gases to be purged from sample lines. Ensure CO/CO<sub>2</sub> readings are zero before proceeding.
30. Check data loggers on back of cone to ensure all numbers are fluctuating. If not, turn both power isolation switches off and then back on to fix the problem.

**Methanol Calibration** – (Approx. 480 seconds for test)

1. Turn pump OFF until ready to run a test.

2. Measure a quantity of methanol into the methanol holder. The amount is not important, but 70–200 g is sufficient. Note weight in Cone Log Book.
3. Place holder in cone with the piezo spark igniter just resting above the methanol.
4. Close all doors.
5. Change scan rate to 2 seconds on 'database' page.

Turn pump ON and bleed off cold trap to release water (bottom front left corner of cone).

7. Check that the O<sub>2</sub> analyzer pressure is registering 108.4 Pa and the % O<sub>2</sub> is registering 20.95 on the 'Misc' screen. Adjust if necessary. Go back to Database screen.
8. Start test by clicking on the green 'Record Test' button. Type in the specimen, material, and mass details and close the window. Ensure baseline database is being used. (The current version in use is Cone Calorimeter Baseline 12-11-2004.trd)
9. The baseline will run for 75 seconds.
10. After the baseline is complete (i.e. time is 0 seconds), press 'ignition' on the hand held controller to start the test. Then continually press the button on the piezo spark igniter whilst slowly pulling the igniter out of the MeOH. When the MeOH begins to burn, press 'ignition' again to record the ignition time on the screen. Remove igniter.
11. After methanol has been burnt and the baseline oxygen has returned to 20.95, end the test by pushing the 'END' key on the keyboard.
12. Pump OFF.

13. Close database pop-up screen, update any mistakes, e.g. wrong mass or ignition time in the database worksheet.
14. Go to methanol worksheet and observe the 'C' factor. It should be between 0.04 and 0.05 but is more commonly 0.043 or 0.045. If the 'C' factor is not in this range, see the troubleshooting section.
15. Save the new 'C' factor. (Flow rate on screen should read  $\sim 0.024$  m<sup>3</sup>/s).
16. Record the 'C' factor in the 'Cone' workbook, as well as any other workbook relevant to the samples being tested.

### 3.3.2.2 Standard Test Procedure

1. Allocate a number to the test specimen and record details in the cone logbook. Typically, the specimen will have a test number such as 225A50. The '225' denotes the sample number, the 'A' is the sample replicate and the '50' denotes the heat flux used. If more than one sample is tested on a



given day, add an additional character to test number, i.e. B, C, D, to signify other replicates.

2. Place test specimens in conditioning cabinet until a stable specimen weight is reached – usually 5-7 days.

**Figure 19: Conditioning Cabinet at  $23\pm 2^{\circ}\text{C}$  and  $50\pm 5\%$  relative humidity**

3. Change soot filter.
4. Carry out a spark igniter check.
5. Set shield in place.
6. Change heat flux by changing the heater temperature if necessary.
7. Ensure temperature has stabilized before proceeding.
8. Remove test specimen from conditioning cabinet.
9. Weigh test specimen and record details in Lab Test Book. Specimen is placed inside an aluminum foil tray and placed in a specimen holder packed to a height of 25 mm below the heater with ceramic fiber blanket (e.g. 2 x kaoboard + kaowool). This height is also 30 mm above the edge of the specimen holder when no edge frame is used. When an edge frame and/or edge frame plus grid is used the specimen should be positioned at a height so that it fits comfortably inside the edge frame.
10. Place specimen in the cone.
11. Go to 'database' screen and ensure scan rate is 5 seconds.
12. Return to the 'misc' screen.
13. Turn pump ON.
14. Bleed off cold trap to release water.
15. Check that the O<sub>2</sub> analyzer pressure and the % O<sub>2</sub> is registering 108.4 Pa and 20.95 respectively and adjust if necessary. (If the screen freezes, click to another screen then back to the 'misc' screen).
16. Check that the laser ratio is 1.0 and adjust if necessary. Return to Database screen.

17. Start test by clicking on the green 'Record Test' button. Type in the specimen, material, thickness, mass, and heat flux details and close the window. Ensure baseline database is being used.
18. The baseline will run for 75 seconds.
19. After baseline is complete (i.e. time is 0 seconds), remove shield and press 'start' on hand held controller when spark igniter begins to spark. This starts the test.
20. Press 'start' again when the specimen has ignited. This records the ignition time.
21. Press 'ignition' on hand held controller to remove the spark igniter from the flames.
22. Some specimens may 'flash' prior to ignition.
23. Record the time at which flashing commenced, as well as the ignition time in the 'Cone' workbook.
24. After the required testing time (varies from specimen to specimen), end the test by pushing the 'END' key on the keyboard.
25. Pump OFF.
26. Set heater shield in place under heater.
27. Close database pop-up screen, update any mistakes, e.g. wrong mass or ignition time in database worksheet.
28. Record any observations during the test in the cone workbook.
29. Change soot filter in readiness for the next test.
30. Remove the specimen and specimen holder from the cone.
31. Test spark igniter in readiness for the next test.

## **Shut Down Procedure**

1. Pump OFF.
2. Shield over.
3. Place ceramic block on load cell.
4. Set temperature to zero. Turn flue heater OFF if in use.
5. Turn cold trap OFF.
6. Laser OFF.
7. Ignition OFF.
8. When temperature has cooled to  $\sim 200^{\circ}\text{C}$ , turn fan OFF and fan control switch to 'manual'.
9. Turn scrubber OFF.
10. Turn purge air OFF.
11. Turn water OFF.

### 3.3.3 Pyrolysis Method in Nitrogen and Low O<sub>2</sub> environment

The same pre-test, methanol, and shutdown procedures were used as the previous section. The standard test procedure was different, as detailed below.

1. Ensure Nitrogen tanks have been filled and connected to system via liquid outlets, allow space in hut to access valves after system has been in use and iced up (see Figure 20).



**Figure 20: Liquid nitrogen and glycol tanks**

2. Turn heater to glycol tank ON and set @ 60°C before calibration.

After Calibration

3. Ensure Red valve behind the cone on wall is shut / off before turning on tanks.

4. Turn on Pressure building valves (Green, see diagram in hut) and liquid exit valves connected to system (Blue).
5. Use personal gas detector to monitor lab oxygen levels.
6. Connect air to automated control valve after removing yellow hose, it has an inlet operating pressure of 2- 6 bar, ensure pressure is less than 6 Bar, regulator should be set to approx 400 kPa.
7. Press mode button for manual (green light off) and up & down arrows for % open position.
8. CAUTION before ON/OFF valve is opened scrubber & fan must be on and all doors shut and sealed.
9. DO NOT open doors until Nitrogen valve is off and oxygen has returned to at least 20 %.

After pressure has built in tanks testing can begin.

1. Allocate a number to the test specimen and record details in the cone logbook. Typically, the specimen will have a test number such as 225A50. The '225' denotes the sample number, the 'A' is the sample replicate and the '50' denotes the heat flux used. If more than one sample is tested on a given day, add an additional character to test number, i.e. B, C, D, to signify other replicates.
2. Place test specimens in conditioning cabinet until a stable specimen weight is reached – usually 5-7 days.
3. Change soot filter.
4. Carry out a spark igniter check if required.
5. Set shield in place.
6. Change heat flux by changing the heater temperature if necessary.

7. Ensure temperature has stabilized before proceeding.
8. Remove test specimen from conditioning cabinet.
9. Weigh test specimen and record details in Lab Test Book. Specimen is placed inside an aluminum foil tray and placed in a specimen holder packed to a height of 25 mm below the heater with ceramic fiber blanket (e.g. 2 x kaoboard + kaowool). This height is also 30 mm above the edge of the specimen holder when no edge frame is used. When an edge frame and/or edge frame plus grid is used the specimen should be positioned at a height so that it fits comfortably inside the edge frame.
10. Place specimen in the cone.
11. Go to 'database' screen and ensure scan rate is 5 seconds.
12. Return to the 'misc' screen.
13. Turn pump ON.
14. Bleed off cold trap to release water.
15. Check that the O<sub>2</sub> analyzer pressure and the % O<sub>2</sub> is registering 108.4 Pa and 20.95 respectively and adjust if necessary. (If the screen freezes, click to another screen then back to the 'misc' screen).
16. Once % O<sub>2</sub> is 20.95 and pressure 108.4 Pa is reached open Nitrogen valve and adjust automated valve by pressing up and down buttons, set to approx 40% open for 6-8% O<sub>2</sub>. Depending on required oxygen level adjust valve percentage.
17. Wait until the oxygen level has reached steady state and adjust automated valve for main adjustment and flow taps for fine adjustment. This takes time as each change will take > 20 sec for the analyzer to respond plus time for pressure variations within the tanks to balance.

18. Work in steps to incrementally adjust the oxygen level using the automated valve until the desired oxygen level is reached.
19. When % O<sub>2</sub> is steady and at required level start test step. Check that the laser ratio is 1.0 and adjust if necessary. Go to Database screen.
20. Start test by clicking on the green 'Record Test' button. Type in the specimen, material, thickness, mass, and heat flux details and close the window. Ensure baseline database is being used.
21. The baseline will run for 75 seconds.
22. After baseline is complete (i.e. time is 0 seconds), remove shield and press 'start' on hand held controller. This starts the test. (As piloted ignition isn't usually required press 'ignition')
23. After test is completed press 'End' to end test and turn OFF nitrogen, update any mistakes or changes and return to Misc.
24. Close shield.
25. Check that O<sub>2</sub> rises from test level eg. 4% to 20 %. When oxygen has returned to atmospheric conditions. Turn pump off and doors can be opened.
26. Glycol tank heater & exit valves can be left on during a day of testing but if left e.g. Over lunch, turn off pressurizing valves to avoid too much blow off and waste of Nitrogen. At completion of days testing, turn off pressurizing valves, exit valves & heater for glycol tank.

### **3.4 TGA-DTSC and FTIR**

The following is a breakdown of the individual experiments conducted with the TGA and FTIR apparatus:

- Combustion conditions
  - Untreated
    - 3 samples x 4 heating rates = 12
  - Treated
    - 3 samples x 4 heating rates = 12
- Pyrolysis Conditions
  - Treated
    - 3 samples x 4 rates = 12

#### **3.4.1 Sample Preparation**

Thermogravimetric analysis requires that the samples being tested be of particle sizes (<150 microns). Since the necessary equipment was not available at the CSIRO Hightt campus, we had to go to the ENSIS in Clayton to use the Wiley mills.

Two saw blades were cleaned with rubbing alcohol in order to remove any oxide buildup or other particles that may have been present on the blades. These were used to dice a 50×50×10 mm sample of untreated pine into 5mm cubes, which were then taken to the ENSIS facility in Clayton.

The Wiley mills were cleaned as thoroughly as possible with a vacuum cleaner and wet towels to remove previous residue buildup. It was essential that the purity of our samples be maintained, given the sensitive nature of TGA. The diced cubes

were then initially run through the 3mm sieve for 20 seconds. The resulting particles were collected and run through the mill again, but now using a 0.75 mm sieve for 2 minutes. To avoid contamination from previous milling, we had to insert our sample immediately into the chute while the mill was running, instead of placing it in the compartment. The samples were run through the 0.75 mm sieve once again for 5 minutes, and finally for 3 minutes. These repetitions were necessary since we required our particles to be in the micron size range, and this enabled us to get the smallest sizes possible.

The trays, blades, and sieves were then thoroughly cleaned, and the same procedure was repeated for the treated sample.

These ground samples contained a wide variety of particle sizes. In order to ensure the effectiveness of the TGA, the ground samples were separated into particular particle sizes using sieves. Using a set of sieves, we had the following sizes separated, as also shown in Figure 21 and Figure 22:

- $>250 \mu$ ,
- $250-150 \mu$ ,
- $150-75 \mu$ , and
- $<75 \mu$ .

Once we had the different particle sizes, it was necessary to perform several pilot tests to work out which would yield optimum results. Tests on the  $<75 \mu$ ,  $150-75 \mu$ , and the  $250-150 \mu$  range were carried out. We wanted to ensure that the physical regime outweighed the diffusion-phase kinetics.



**Figure 21: Untreated Timber samples for TGA**



**Figure 22: Treated Timber samples for TGA**

### **3.4.2 Thermogravimetric Analysis and Infrared Spectroscopy**

The TGA investigations were divided into two main sections: combustion and pyrolysis. While doing combustion, an airflow rate of  $100 \text{ ml min}^{-1}$  was used, and for pyrolysis work,  $100 \text{ ml min}^{-1}$  of  $\text{N}_2$  was used. Alumina sample pans were used to hold the samples.

A calibration of the apparatus was required before the experimental work was started. In order to do this, the furnace was opened, and the reference and sample pans were emptied and replaced if necessary. The furnace was closed and the weights were tared with the empty pans. Once the taring process was over, the furnace was opened and approximately 20mg of aluminum oxide was put in the reference pan. An equal mass of the 150-75 micron timber sample was placed in the sample pan. It was necessary that the two masses be within 5% of each other. The furnace was closed with the samples inside.

For most of the combustion testing, the starting temperature was set to be  $50^\circ\text{C}$ , and the final temperature  $600^\circ\text{C}$ . Different heating rates of  $7.5$ ,  $10$ , and  $15^\circ\text{C min}^{-1}$  were used as the ramp rates. These low heating rates were chosen so as to

“suppress the effects of heat and mass transfer inside the samples as much as possible”, and thus being able to obtain the overall chemical degradation characteristics (Kashiwagi, et al 1987).

For pyrolysis experiments, the final temperature was set to 1 200°C, with the same heating rates and starting temperature as the combustion tests. These tests were carried out to a higher temperature because in the pilot tests, we observed a second peak that appeared later in the mass loss percentage graphs.

In order to collect FTIR data, the gases produced by either pyrolysis or combustions were transferred to the FTIR via a heated SS tube and analyzed in a heated FTIR cell with a path-length of 180mm. The gases were quantified using the classic least squares methodology within the Omnic Quantpad software. A calibration run consisting of upto 10 standards was performed before the actual experiment, and used to generate the standard curves within Quantpad.

### **3.5 Porosity**

The porosimeter was not in working order during the course of this project, and as a result, we were unable to collect porosity data.

## **4 Data Analysis**

As seen in the Methodology section, a variety of equipment was used to obtain data for the investigation at hand. This section discusses techniques used to analyze the raw data. The information obtained from this data was discussed in the next section, Results and Analysis.

### **4.1 Cone Calorimeter**

The cone calorimeter was used to collect a large amount of data. Both combustion and pyrolysis of treated as well as untreated pine were conducted. From the cone, it was possible to obtain curves for mass loss, mass loss rate, heat release rate, effective heat of combustion, as well as the carbon monoxide and carbon dioxide emissions.

Even though no further calculations were done with this data, it was used on a qualitative basis to gain a deeper understanding of the materials and their interactions. The differences in conditions such as pyrolysis viz. combustion were presented in the following sections.

In addition, effective heat of combustion and residual mass data obtained from cone tests were also compared to literature values.

### **4.2 TGA**

Thermogravimetric analysis data was used to generate kinetics data for the reactions occurring in combustion and pyrolysis of treated and untreated pine. The model used to calculate these parameters was the one developed by Broido (Broido 1969).

The reaction order was assumed to be between 0 and 1 (Hirata, et al 1991) for the different stages of the pine's thermal degradation. The equation used to calculate the activation energy was given by:

$$\ln\left[\ln\left(\frac{1}{y}\right)\right] = -\frac{E_a}{R} \frac{1}{T} + \ln\left(\frac{R}{E_a} \frac{Z}{\beta} T_m^2\right)$$

where  $y$  is the fraction of initial molecules not yet decomposed.  $T_m$  is the temperature of maximum reaction rate,  $\beta$  is the rate of heating,  $Z$  is the frequency factor and  $E_a$  is the activation energy.

For the various stages of the reaction,  $\ln[\ln(1/y)]$  was plotted against  $1/T$  from the TG curves. Linear plots were obtained in each of the cases with slopes of  $E_a/R$ , which eventually yielded the activation energies of each stage of the reaction. These activation energies are compared to literature values in the approaching sections.

### **4.3 FTIR**

Gases released during the reactions discussed above were captured and analyzed by the FTIR spectrum. These gas emissions were plotted with the mass loss rate curve in order to better represent gas release with respect to the reactions going on. This data was also compared to published data about the combustion of untreated wood.

## **5 Results and Analysis**

The goal of this section is to analyze the data obtained and to discuss it with reference to the aim of this investigation, which was to obtain better understanding of the properties and behavior of fire retardant treated wood. Comparisons will be presented between untreated and treated wood under both pyrolysis and combustion conditions. Data obtained in this investigation will also be discussed and referenced to published values found in journals and texts.

### **5.1 Kinetic Parameters**

Before specific kinetics could be computed or any models applied, a rate of reaction for the degradation of wood had to be specified. It seems to be widely agreed that the individual mechanisms that occur during the burning of wood are non-reversible first order reactions (Orfão 1992).

According to Liu, et al (2002), the evaluation of kinetic parameters in homogeneous reactions are important since they are considered to be indicative of the reaction mechanism. However, in the case of heterogeneous reactions which take place in the solid state, these parameters lose their relevance because the concepts such as reaction order or concentration are more complex.

It was also evident from the literature that activation energy values depended heavily on various experimental factors such as sample size, particle size and distribution, heating rate, presence of impurities in the sample, and gaseous atmosphere in and around the sample. This lead to the question whether experimentally determined kinetic parameters had any relevance to practical application. The 'kinetic compensation factor' and other such theories exist in order to take the aforementioned points into consideration, but their application in this investigation was beyond the scope of this paper.

The activation energy of different stages of the respective combustion or pyrolysis of untreated and treated samples was found using data obtained from the thermogravimetric analysis. Activation energies using the Broido method (Broido 1969) were calculated as shown in Table 3-Table 6:

**Table 3: Activation Energy [kJ mol<sup>-1</sup>] of Combustion of Treated Pine at 3 different heating rates**

	Temp Range °C	7.5°C min <sup>-1</sup>	10°C min <sup>-1</sup>	15°C min <sup>-1</sup>
<b>Phase I</b>	205-340	44.0	28.5	31.7
<b>Phase II</b>	490-660	27.2	28.4	29.2
<b>Phase III</b>	660-700	20.7	25.2	25.6

**Table 4: Activation Energy [kJ mol<sup>-1</sup>] of Pyrolysis of Treated Pine at 3 different heating rates**

	Temp Range °C	7.5°C min <sup>-1</sup>	10°C min <sup>-1</sup>	15°C min <sup>-1</sup>
<b>Phase I</b>	190-340	37.7	28.5	33.8
<b>Phase II</b>	570-930	3.6	3.1	-

**Table 5: Activation Energy [kJ mol<sup>-1</sup>] of Combustion of Untreated Pine at 3 different heating rates**

	Temp Range °C	7.5°C min <sup>-1</sup>	10°C min <sup>-1</sup>	15°C min <sup>-1</sup>
<b>Phase I</b>	225-375	61.6	70.0	57.6
<b>Phase II</b>	375-460	31.4	30.5	29.5

**Table 6: Activation Energy [kJ mol<sup>-1</sup>] of Pyrolysis of Untreated Pine at 3 different heating rates**

	Temp Range °C	7.5°C min <sup>-1</sup>	10°C min <sup>-1</sup>	15°C min <sup>-1</sup>
<b>Phase I</b>	225-400	58.4	49.8	57.6

An earlier 'phase' in both the combustion and treated pyrolysis were detected around 80-150°C, but those are results of the vaporization of bound and unbound water molecules, and were caused by a reaction occurring in the wood itself. Thus, these were not considered as degradation mechanisms of the wood, and were ignored for the purposes of this investigation.

Even though no published data about activation energies of treated pine was found, activation energy data for the combustion of untreated wood does exist. However, there were many factors to consider, because a seemingly intrinsic property of a material, the activation energy of wood is multifaceted in its dimensions. Firstly, many varieties of woods exist, and each of them can vary tremendously from the others in all its physical properties. This means for the comparison to be valid, the same family of wood should be chosen. One could also think that since wood is largely composed of celluloses and lignin, their activation energies could be compared directly. This, however, cannot be done with precision since the individual energy barriers posed by cellulose, hemicellulose, and lignin are not of the same nature or magnitude as that posed by the barriers caused from their synergies when in one substance. These three major compounds interact while burning, and thus cannot be modeled on an individual component basis.

A second factor considered while comparing activation energies is the model used to calculate these kinetic factors. A very large number of such models that can evaluate kinetic factors exist; however, each of them is better suited to different situations that favor that particular method. As recommended by Dr. Donovan Marney of CSIRO, the Broido method seemed to be best suited to evaluate kinetic parameters of cellulosic substances for data obtained by thermogravimetry. This is demonstrated by Broido (1969) himself as he discusses thermal analyses of wood and cellulose in his paper.

In one of their studies Gao et al. (2004) used Chinese Larch with thermogravimetric equipment to study its kinetics. Larch is of the same family *Pinaceae* as is *Pinus Radiata*, the material investigated in this report. In addition, Gao et al. employed the Broido method to determine the activation energy for each of the stages of the degradation reaction. Even though the genus and species of wood tested, as well

as the testing conditions varied somewhat, a comparison between the two can be deemed acceptable. Table 7 shows the activation energy obtained by Gao:

**Table 7: Activation energy data of Chinese Larch [Gao et al.]**

	<b>Temp Range / °C</b>	<b>Mass Loss / %</b>	<b><math>E_a</math> / kJ mol<sup>-1</sup></b>
<b>Phase I</b>	240-290	4.8	81.0
<b>Phase II</b>	290-365	51.5	116.0
<b>Phase III</b>	365-480	25.3	15.8
<b>Phase IV</b>	480-515	9.6	62.4

Even though Gao used the same Broido model to evaluate these activation energies, their techniques of calculation differed in terms of how individual phases were divided. For the sake of comparison, kinetic parameters obtained in this investigation were recalculated using a similar phase breakdown scheme as Gao. In this, the first phase, 240-290°C occurred before the first DTG peak, and the equivalent region, from Figure 23 was 190-260°C. Phase II lead up to the peak, and can be represented by 260-326°C in Figure 23. Phase III can be represented by 327-430°C, and the final Phase IV, which included the second peak ranged over 430-464°C.

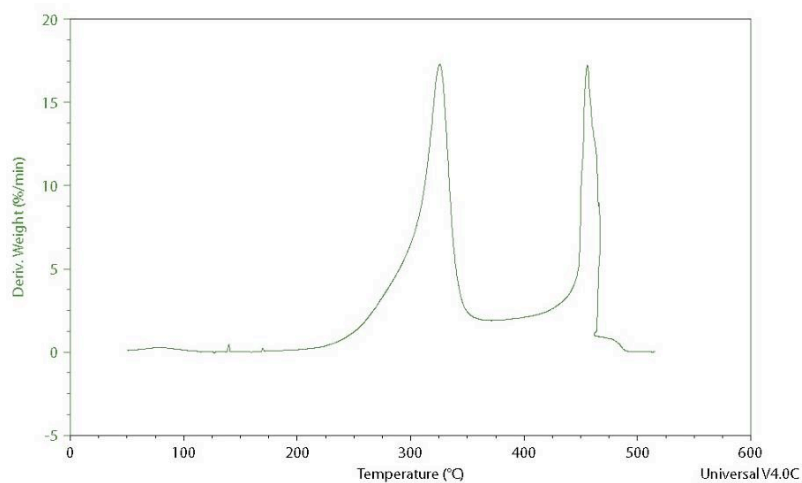


**Figure 23: Derivative Weight Loss Curve for Untreated wood, 10°C min<sup>-1</sup>**

The recalculated activation energies are presented in Table 8:

**Table 8: Activation energies recalculated in 4 phases**

	<b>Temp Range / °C</b>	<b>Mass Loss / %</b>	<b><math>E_a</math> / kJ mol<sup>-1</sup></b>
<b>Phase I</b>	190-260	3.9	21.4
<b>Phase II</b>	260-326	38.5	81.9
<b>Phase III</b>	327-430	34.3	24.4
<b>Phase IV</b>	430-464	12.3	59.4

The recalculated activation energies did not match those of Gao's per se, however, they were comparable, and a similar trend was observed. The activation energy of the first phase, where char was presumed to be forming was relatively low compared to the activation energy of the second phase. Likewise, an increase was noted from the third to the fourth phase, as more energy may have been required to collapse the char. These trends can be better observed in Figure 24.

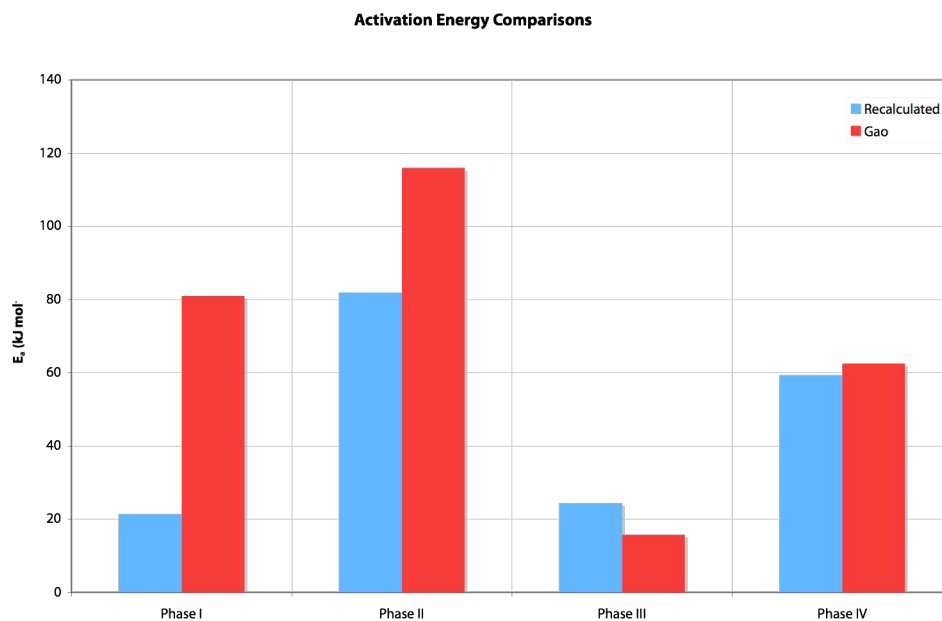


**Figure 24: Comparison between recalculated and Gao's activation energies**

Another reason why we would not have expected the two sets of data to be identical was the difference in thermal experimentation techniques. The particle size of the sample used in the TGA apparatus has a big impact on the results obtained. A particle size range of 150-250 $\mu$  was used during this investigation; such information is not available for Gao's experiments.

According to the Shafizadeh (1984) and White & Dietenberger (2001), the values obtained for the activation energies were within acceptable ranges for both combustion and pyrolysis of untreated wood. Acceptable ranges of 66-124 kJ mol<sup>-1</sup> for combustion of untreated wood and 63-147 kJ mol<sup>-1</sup> for pyrolysis in nitrogen were stated.

Greg Griffin from CMIT, CSIRO also calculated invariant kinetic parameters (IKP) for untreated and treated wood in standard and low oxygen atmospheres.

Figure 25 and Figure 26 show the TGA results (at 7.5°C min<sup>-1</sup>) for wood pyrolysis and combustion respectively (residual mass fraction plotted vs. temperature (°C)). All experimentally measured mass loss curves were fit using a model of two, independent, first-order reactions. The equations used for this can be found in the paper published by Griffin, et al in the Journal of Fire Sciences, 2005 (pp303-328). The model fit was performed using data up to 600°C only. Table 9-11 show the calculated reaction parameters.

From the TGA plots in Figure 25, it is evident that the residual mass percent was much higher for the treated wood, which is also shown by the higher  $\gamma_{\text{inert}}$  values in Table 9. The same trend can be observed with the combustion of both treated and untreated wood, where there is also 20% more residual mass for the treated wood. This is a good sign that the fire retardant is effective, since it is preventing the wood from burning off. Figure 25 also shows that the majority of the mass is lost between 300-400°C; this corresponds to the FTIR data where the highest emission

of sulfur dioxide and carbon dioxide were detected, leading us to believe the a large part of the breakdown of wood occurs around this temperature range.

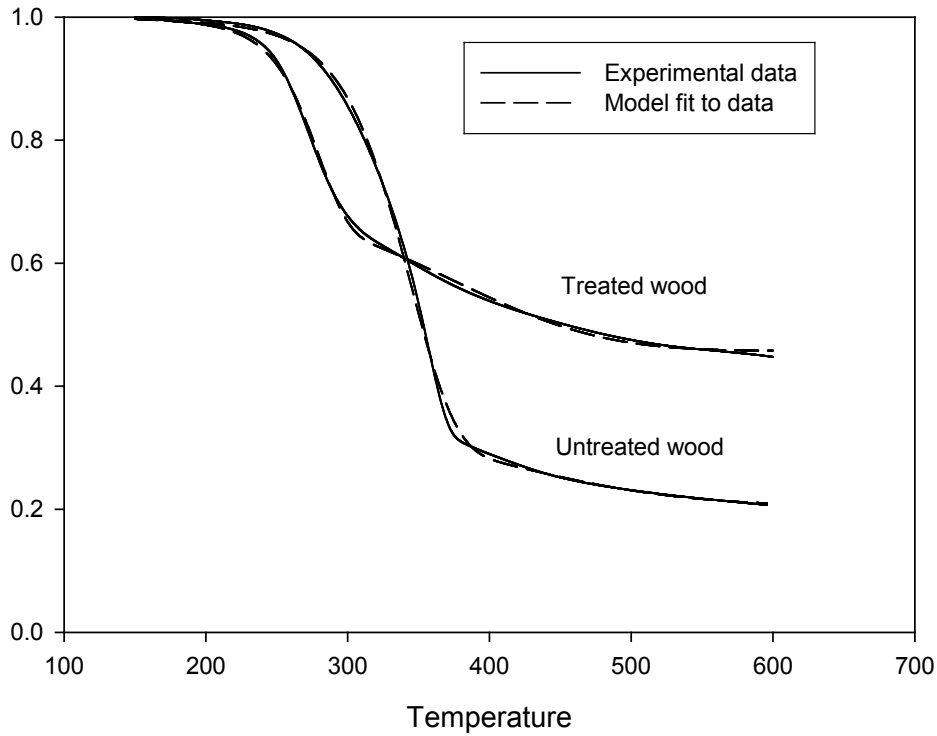


**Figure 25: Mass-loss curves for pyrolysis of treated and untreated wood heated at 7.5°C min<sup>-1</sup>**

**Table 9: Calculated pyrolysis parameters of treated wood**

Heating rate (°C/min)	1 <sup>st</sup> stage			2 <sup>nd</sup> stage			$\gamma_{inert}$
	$\gamma_1$	$z_1$ (min) <sup>-1</sup>	$T_{a,1} \cdot 10^3$ (K)	$\gamma_2$	$z_2$ (min) <sup>-1</sup>	$T_{a,2} \cdot 10^3$ (K)	
7.5	0.296	$12.4 \times 10^{10}$	14.7	0.246	$2.35 \times 10^1$	3.93	0.458
10	0.297	$29.6 \times 10^{10}$	15.1	0.247	$2.81 \times 10^1$	3.88	0.457
15	0.295	$183 \times 10^{10}$	15.9	0.250	$4.00 \times 10^1$	3.85	0.455

**Table 10: Calculated pyrolysis parameters of untreated wood**

Heating rate (°C/min)	1 <sup>st</sup> stage			2 <sup>nd</sup> stage			$\gamma_{inert}$
	$\gamma_1$	$z_1$ (min) <sup>-1</sup>	$T_{a,1} \cdot 10^3$ (K)	$\gamma_2$	$z_2$ (min) <sup>-1</sup>	$T_{a,2} \cdot 10^3$ (K)	
7.5	0.631	$1.14 \times 10^8$	12.4	0.163	4.13	3.11	0.206
10	0.632	$1.14 \times 10^8$	12.3	0.157	6.08	3.21	0.212
15	0.646	$0.705 \times 10^8$	11.9	0.142	2.77	2.82	0.211

The activation temperatures,  $T_{a,i}$ , were also higher for the treated pine in both the first and the second stages. This led to consequently higher pre-exponential factors,  $Z_i$ .

The residual mass percent was plotted against the temperature for the combustion reactions in Figure 26. Once again, it can be observed that the treated wood had a higher residual mass fraction than the untreated wood, once again underlining the effectiveness of the fire retardant treatment.

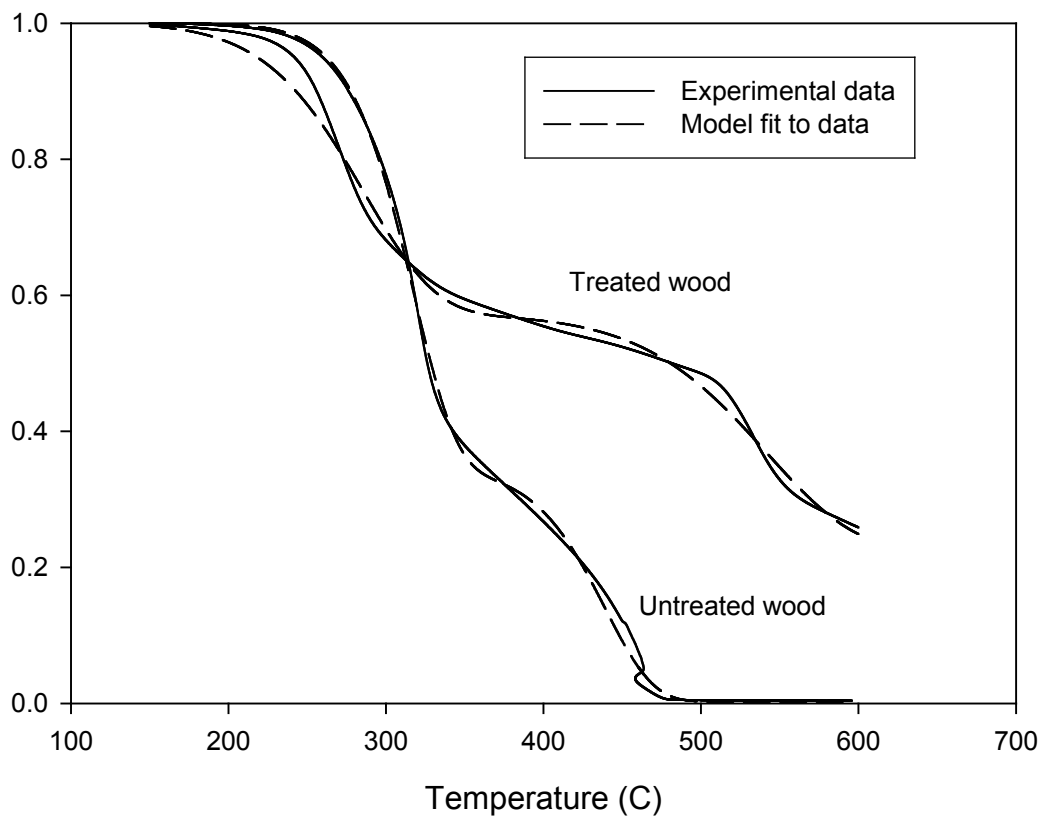


**Figure 26 : Mass-loss curves for combustion of treated and untreated wood heated at  $7.5^{\circ}\text{C min}^{-1}$**

The kinetic invariant parameters for the oxidation reactions were calculated and were found to be as follows:

**Table 11: Calculated oxidation parameters of treated wood**

Heating rate (°C/min)	1 <sup>st</sup> stage			2 <sup>nd</sup> stage			$\gamma_{inert}$
	$\gamma_1$	$z_1$ (min) <sup>-1</sup>	$T_{a,1} \cdot 10^3$ (K)	$\gamma_2$	$z_2$ (min) <sup>-1</sup>	$T_{a,2} \cdot 10^3$ (K)	
7.5	0.428	$2.89 \times 10^4$	6.83	0.347	$2.44 \times 10^5$	11.8	0.225
10	0.451	$1.23 \times 10^4$	6.28	0.337	$65.3 \times 10^5$	14.2	0.212
15	0.456	$1.40 \times 10^4$	6.37	0.371	$0.899 \times 10^5$	11.3	0.173

**Table 12: Calculated oxidation parameters of untreated wood**

Heating rate (°C/min)	1 <sup>st</sup> stage			2 <sup>nd</sup> stage			$\gamma_{inert}$
	$\gamma_1$	$z_1$ (min) <sup>-1</sup>	$T_{a,1} \cdot 10^3$ (K)	$\gamma_2$	$z_2$ (min) <sup>-1</sup>	$T_{a,2} \cdot 10^3$ (K)	
7.5	0.654	$7.54 \times 10^8$	12.9	0.344	$3.50 \times 10^9$	16.7	0.002
10	0.659	$9.84 \times 10^8$	13.0	0.340	$11.6 \times 10^9$	17.4	0.001
15	0.669	$9.28 \times 10^8$	12.9	0.326	$69.5 \times 10^9$	18.5	0.005

Unlike the pyrolysis reactions, the untreated wood had higher activation temperatures for both stages than the treated wood. It can be inferred that oxidation of treated wood occurs more readily than oxidation of untreated wood, yet pyrolysis of untreated wood occurs more readily than untreated wood.

## 5.2 FTIR Analysis of Gaseous Emissions

A great amount of importance is assigned to the smokes and gases produced by burning wood. These products of burning wood are the major contributors to death in approximately thirty percent of cases in combination with heart disease, BAC, and burns. In addition, smoke can obscure visibility in closed spaces, which not only hinders the work of firefighters, but also causes higher panic and retards escape (Tang, et al 1968).

A wide variety of compounds are found in wood smoke, which may include gases, solid particles, and droplets of water. The individual concentrations of each these components depends on the stage of the burn and factors such as fire exposure, oxygen and moisture present, the species of wood, and any other treatments that may have been applied to the wood. One approach that may be used to estimate the hazard of wood smoke is to find toxicity data for the individual smoke components. This however neglects synergistic effects and is not as valuable (Wood Eng Handbook, 2000).

According to Holmes (1967), more smoke is produced under non-flaming combustion than under flaming combustion. The products from burning wood under flaming combustion are carbon dioxide, water, and ash. Incomplete combustion also leads to the presence of other gases and vapors such as carbon monoxide, methane, formic acid, acetic acid, glyoxal, and saturated and unsaturated hydrocarbons (Wagner 1972). There is no standardized test method to determine the combustion products that are given off from wood or other materials in a real-life fire situation. The majority of studies on the toxicity of combustion products conclude that carbon dioxide is the dominant hazardous gas that results from burning wood, followed by carbon monoxide, and the resulting oxygen depletion (Birky 1973, Einhom et al 1974, O'mara 1974). On the other hand fire retardants lead to low-flaming combustion, resulting in more smoke development than in the flaming combustion of untreated wood.

## 5.2.1 FTIR Data

### 5.2.1.1 Combustion of Untreated pine

Figure 27 is a plot of the gases evolved during the combustion of untreated pine, overlaid with the derivative weight loss curve. There was clearly some correlation between gas emission peaks and the MLR peak.

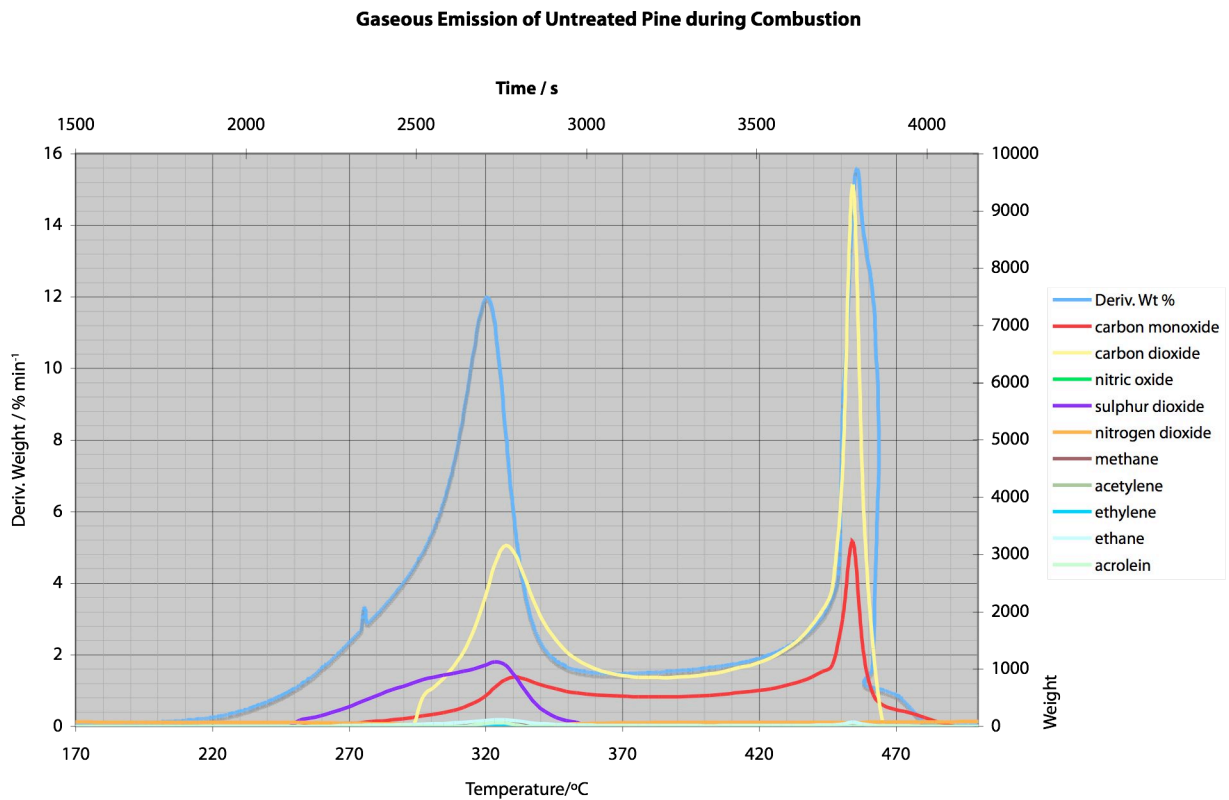


**Figure 27: Gases evolved during the combustion of untreated wood, overlaid with MLR**

Table 13 outlines the data obtained from the infrared spectroscopy for the combustion of untreated pine. The gas given off in the highest quantity was sulfur dioxide, followed by carbon dioxide, carbon monoxide, ethane, methane, and acrolein. Trace amounts of acetylene were emitted in the 300-500°C range. Extremely low amounts of nitrogen dioxide were observed throughout the whole

process, including pre-ignition, which lead us to believe that it may have been present in the environment at that time. The presence of nitrogen oxides in the decomposition is still under investigation, and is currently being researched at CMIT CSIRO.

**Table 13: Gas emission data for combustion of untreated pine**

Temperature (°C)	Description
250	Emission of sulfur dioxide begins
270	Emission of carbon dioxide begins
300	Emission of carbon monoxide begins
330	The following gases peak (in increasing quantity): <ul style="list-style-type: none"> <li>- acrolein</li> <li>- methane</li> <li>- ethane</li> <li>- carbon monoxide</li> <li>- carbon dioxide</li> <li>- sulfur dioxide</li> </ul>
350-440	Lower emissions of sulfur dioxide, carbon dioxide, carbon monoxide, ethane, and acrolein continue
455	A second and larger peak of the following gases occurs (in increasing quantity) <ul style="list-style-type: none"> <li>- acrolein</li> <li>- ethane</li> <li>- carbon monoxide</li> <li>- carbon dioxide:</li> <li>- sulfur dioxide</li> </ul>
> 465	Gas emission rapidly drops out to zero

Compared to Table 1, which outlines the breakdown of the combustion of wood, there is a high level of similarity with the data obtained. As per what White and

Dietenberger (2002), Babrauskas (2001), Fang (1966), Shafizadeh (1984), LeVan (1990), and Kozlowski (2001) have said, exothermic reactions begin in the 200-260°C range, and large amounts of gases are given off between 275-280°C; gases in higher quantity are given off after 300°C. The data obtained follows the same trends.

From Figure 28 it was also apparent that two main reactions govern the combustion of wood, as shown by the two peaks. It was likely the first peak is caused by the release of volatiles, followed by the formation of char. The second peak was a result of the breakdown of the char layer, which trapped many volatiles, leading to a higher amount of evolution of combustible gases.

Since combustion of untreated pine was also carried out in the cone calorimeter, we compared those data with the FTIR data. Figure 28 shows the heat release rate curve superimposed onto the gas emission data. It was noteworthy to observe that the peaks in the heat release rate curve coincide with the peaks when the highest amounts of gases were released. This further added to the concept that the combustion of wood occurs in a two-step reaction.

The reason the peaks did not coincide perfectly is because the data was obtained from two different instruments, and thus, the same scales were not used in the axes of the graph. This phenomenon also aided in illustrating the fact that the behavior of a material changes slightly when tested in a cone calorimeter viz. thermal analysis. A large sample piece of 50×50mm pine was used in cone tests, whereas ~10mg of finely ground pine was used in the TGA apparatus. This addresses one of the problems faced in fire testing: that material properties are not always a uniform function of scalability. Nonetheless, since data from one standardized source is not available, it is also possible that the kinetics of combustion is a cause for this offset.

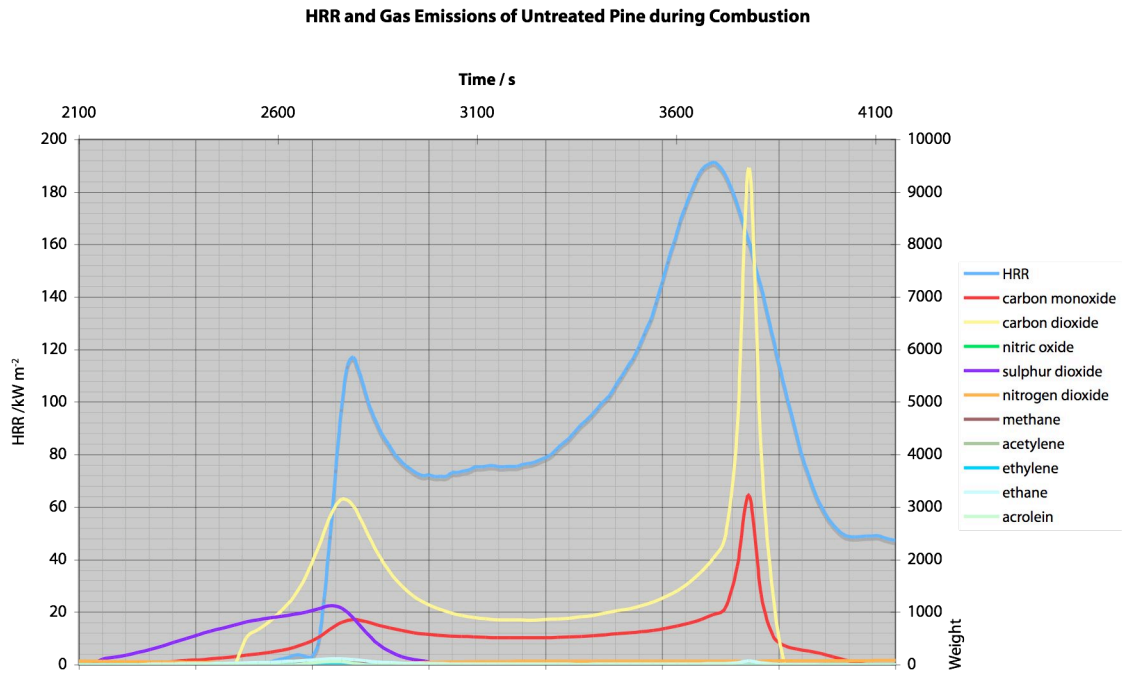


**Figure 28: Heat Release Rate data overlaid with gas emission data**

### 5.2.1.2 Pyrolysis of Untreated pine

Burning of wood in low/oxygen-free environments has not been studied as much in depth as the combustion of wood, and as a result, fewer models exist to detail the breakdown of wood in such conditions.

A plot of gas emissions that occurred during the pyrolysis of pine is shown in Figure 29. As noticed during the combustion of pine, the weight derivative curve overlapped with the gas peaks. Sulfur dioxide, carbon dioxide, and carbon monoxide, respectively, were the gases emitted in the largest quantities. Trace amounts of nitric oxide and nitrogen oxide were also found throughout the process, once again leading us to believe they were not a result of the pyrolysis, but in fact present in the environment. It was suggested that since a nitrogen environment was used to conduct the pyrolysis tests, the nitrogen reacted with air

in the atmosphere to form nitric compounds. This however may not have been the case since the fixation of nitrogen requires higher temperatures. Small quantities of carbon monoxide were also detected around 50°C.

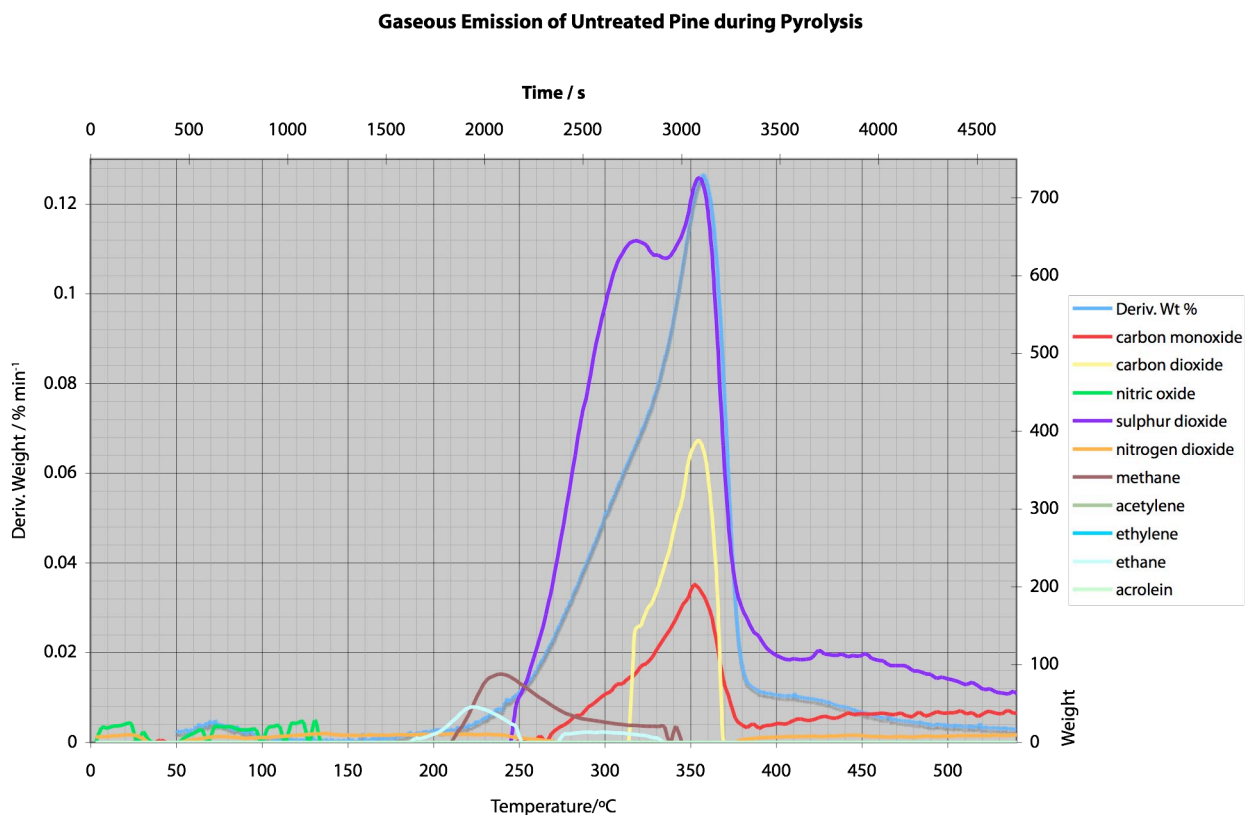


**Figure 29: Plot of gases evolved during pyrolysis of untreated pine, overlaid with MLR curve**

Unlike combustion, it seemed that the pyrolysis of wood can be modeled by one reaction, as suggested by the single MLR peak at 355°C. However, this main reaction spanned longer over nearly 170° whereas the combustions peaks ranged 160° and 50°. It also showed a slower rate of escalation than the combustion reactions.

Table 14 outlines the gases evolved at different stages of pyrolysis.

**Table 14: Gas emission data for pyrolysis of untreated wood**

Temperature (°C)	Description
180	Emission of ethane begins
210	Emission of methane begins
230-40	Ethane and methane emissions peaks
250	Emission of sulfur dioxide begins
260	Emission of carbon monoxide begins
270	First sulfur dioxide peak occurs and second ethane emission (larger) peak occurs
315	Emission of carbon dioxide begins
355	Peaks of the following gases occurs (in increasing quantity) - carbon monoxide - carbon dioxide - sulfur dioxide
> 400	Carbon monoxide and sulfur dioxide emissions drop to ~15% and remain steady until 600°C, and then disappear

Two pyrolysis tests were conducted for untreated wood; the results were almost identical except that in the second test carbon dioxide emissions were detected and the first one had no traces of carbon dioxide. It is normally expected that no carbon dioxide would be produced during pyrolysis due to the lack of oxygen, however depending on the test methods, different results have been reported in the literature.

Nonetheless, the data presented in Table 14 is in agreement with the findings of Browne (1958), who also reported the presence of carbon dioxide in his study. He

also stated that combustible gases and vapors are evolved from 280°-500°C, which was in agreement to our findings.

### ***5.2.1.3 Combustion and Pyrolysis of Burn-X Treated pine***

Similar plots for the combustion and pyrolysis of pine treated with the Burn-X fire retardant treatment were created. Once overlaid with the mass loss rate curves, it was clear that the most gases were evolved at peaks when most mass was lost.

Even though there were differences between how treated and untreated pine burn, there were also a few similarities between the two sets. Combustion of treated pine had two main peak emissions like its untreated counterpart, and pyrolysis of treated pine lead to only one main peak, as did its untreated counterpart. From this, it was determined as the inherent property of wood that combustion degradations can be broken down into two reactions where gases were given off, whereas pyrolysis reactions occurred only in one phase.

The total amount of gases evolved from combustion was much larger than the amount of gas given off during pyrolysis. For untreated pine, peak combustion gas emissions were more than ten times higher than peak pyrolysis emissions. Likewise, the peak combustion gas emissions for treated pine were five-fold larger than those detected from peak pyrolysis gas emissions. This likely could have been due to the fact that gases in the presence of oxygen react more readily with compounds evolved from wood than they could in a nitrogen-rich environment.

Figure 30 and Figure 32 show the plots obtained from FTIR of Burn-X treated pine.

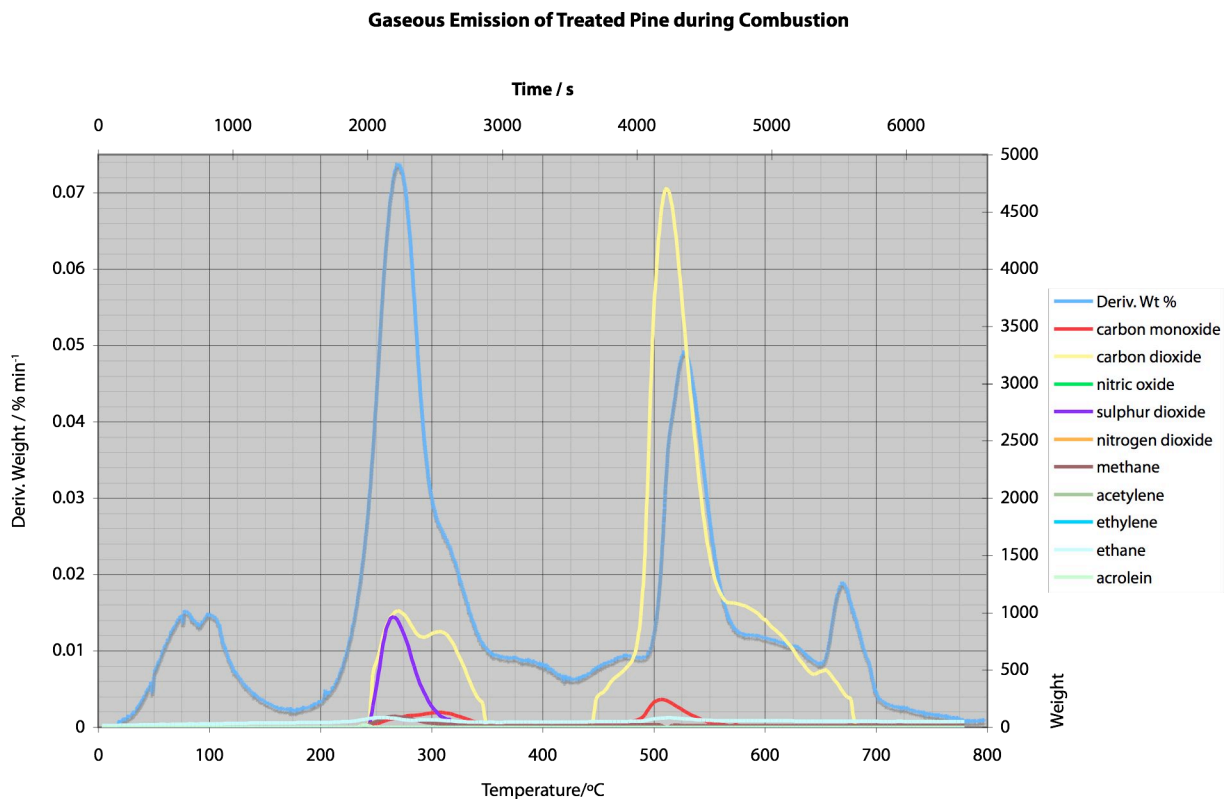


**Figure 30: Plot of gases evolved during the combustion of Burn-X treated pine; overlaid with MLR**

Carbon dioxide and sulfur dioxide were the two gases evolved in the largest quantity during the combustion of treated pine. Small quantities of carbon monoxide were also given off around 270°C and 520°C, which represented the two main reaction peaks. The first peak (25-150°C) may be ignored as far as kinetics of treated pine are concerned since it could be seen no gases were evolved, and thus no reactions took place. The presence of that peak could be attributed to moisture content loss from the wood sample.

The heat release rate (obtained from cone calorimetry) of Burn-X treated pine was also plotted with the gases evolved, and is shown in Figure 31.

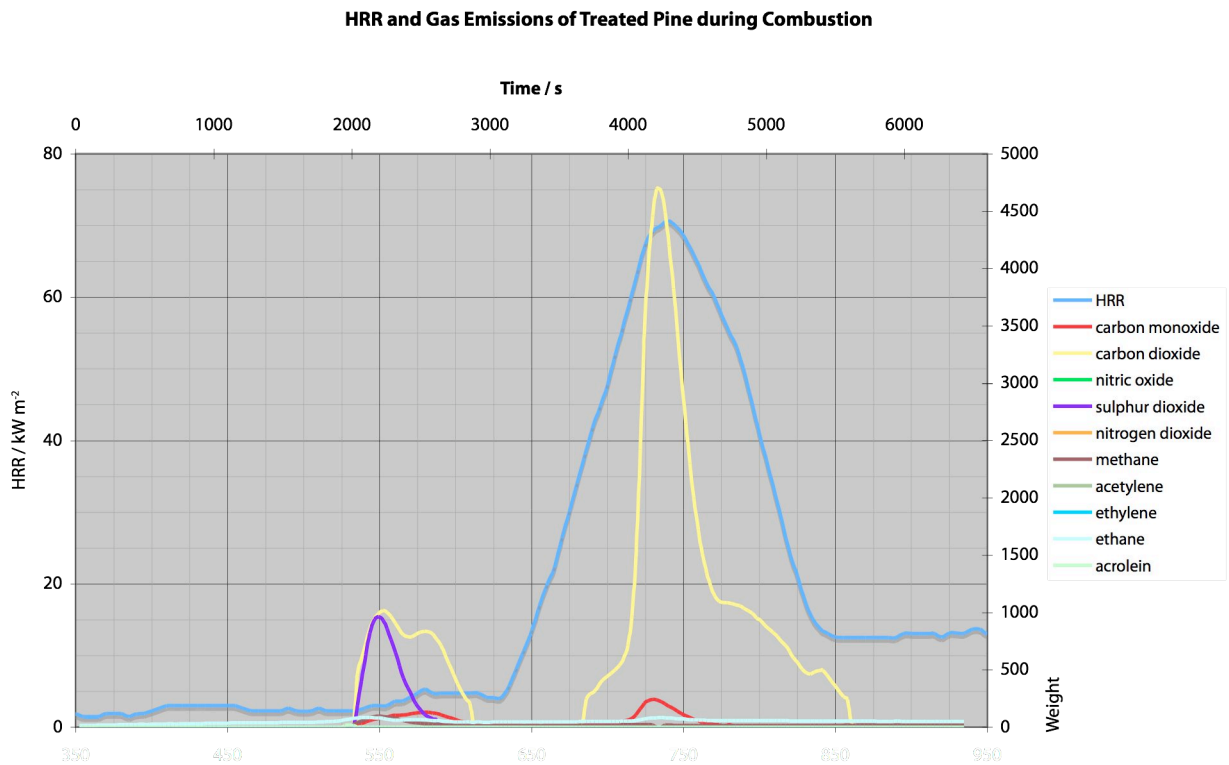


**Figure 31: Heat release rate curve and gaseous emissions during combustion of treated pine**

As with the mass loss rate curve, an overlap of when the highest amount of gases were given off overlaps with when the peak heat release rate occurred.

However, it was interesting to note that even though a smaller peak at around 2100 s occurred where a small amount of CO, CO<sub>2</sub> and SO<sub>2</sub> were evolved, there was no peak detected in the rate of heat release. A second peak around 4150 s where a larger quantity of mainly CO<sub>2</sub> and CO was evolved was where a peak in heat release rate occurred.

Sulfur dioxide emissions were only detected between 2000-2800s, when there was no peak in heat release rate. This aided in providing insight on the behavior of the treated pine, and establishing a relationship between the kinetics of the material and its physiochemical behaviors.

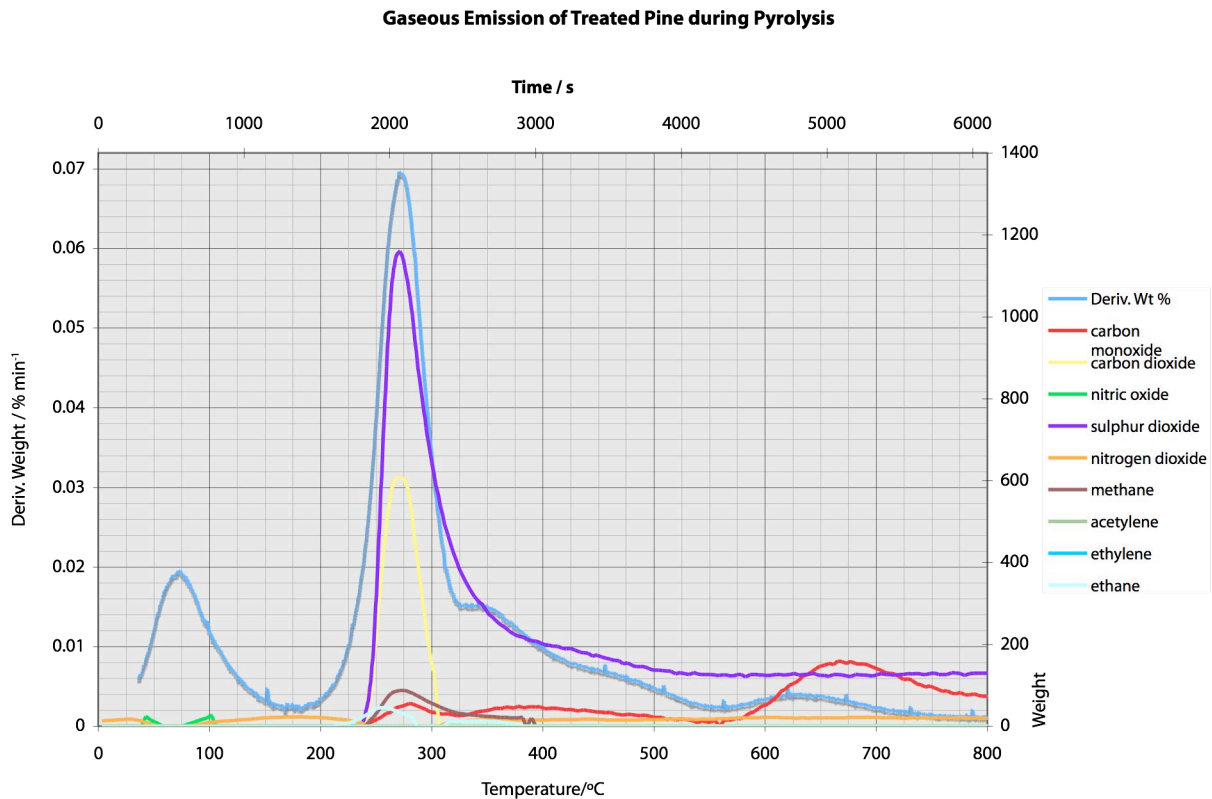


**Figure 32: Plot of gaseous emissions from pyrolysis of Burn-X treated pine; overlaid with MLR**

Unlike the untreated samples where the gases between the combustion and pyrolysis conditions were the same, the gases evolved changed for the treated pine samples. Relatively, more sulfur dioxide was given off than carbon dioxide during pyrolysis, which was the opposite of what occurred during combustion. In addition, methane and ethane were also given off during pyrolysis. Another difference to note is that gases were still being given off after the main peak terminated in pyrolysis, as opposed to in combustion where gas emissions strictly follow the MLR peak. Almost a second 'peak' can be noticed after 600°C where carbon monoxide emissions rose. Since this gas emission data can be used to determine the safety or hazards of the fire retardant, the second carbon monoxide peak would be an important area to investigate.

#### 5.2.1.4 Overall comparison of gaseous emissions

For each of the plots previously discussed, an integration was carried out for each gas to calculate the total amount that was given off for each situation. This information is shown in Table 15.

**Table 15: Total gas emissions (mg g<sup>-1</sup>)**

Gas emitted	During combustion		During Pyrolysis	
	Untreated	Treated	Untreated	Treated
<i>Carbon monoxide</i>	33 547	6 485	5 066	19 722
<i>Carbon dioxide</i>	75 634	107 154	3 899	6 068
<i>Nitric oxide</i>	0	0	492	149
<i>Sulfur dioxide</i>	16 182	9 431	22 995	52 548
<i>Nitrogen dioxide</i>	10 313	0	1 053	4 690
<i>Methane</i>	602	3 431	1 591	1 591
<i>Acetylene</i>	171	0	0	25
<i>Ethane</i>	1 775	10 577	666	808
<i>Acrolein</i>	218	52	0	0

Looking at these data, no evident trend that unified gaseous emission with respect to the type of wood or environment it was burned was apparent. For example, it could be seen that while more carbon monoxide was produced during the combustion of untreated pine, the same did not hold true for pyrolysis conditions, where in fact the treated pine produced more carbon monoxide. In the case of carbon dioxide, it seemed that treatment to the pine increased the amount of CO<sub>2</sub> released during both pyrolysis and combustion.

Another interesting observation to be noted was that no acrolein was detected during pyrolysis of either treated or untreated pine. This could be attributed to the fact that the formation of acrolein requires the presence of oxygen during the combustion of wood. Likewise, it could be observed that no nitric oxide was detected during either the combustion of treated or untreated pine. It could be assumed that the NO was formed because of the nitrogen-rich environment in

which pyrolysis experiments were conducted; therefore eliminating the presence of any NO in combustion experiments.

These data can also be used to evaluate hazards associated with the treatment. Looking at the production of carbon monoxide during pyrolysis, the treated pine had an almost 400% increase in CO emission compared to the untreated pine. Pre-flashover fires have a very limited amount of oxygen present, and it is in these cases where pyrolysis of materials occurs. If this treated wood were to be considered for use as a building material, the high amounts of CO would surely present a health and safety hazard. On the other hand, since accidental fires do comprise primarily of combustion, it is noteworthy that the treated specimen emitted less than 20% CO than its untreated counterpart.

Similarly, the amount of sulfur dioxide emitted could be an indicator of how environmentally sustainable the treatment is. During pyrolysis, a relatively higher amount of SO<sub>2</sub> was emitted from the treated sample, while a much lower amount was detected in the combustion experiments.

### **5.3 Cone Calorimetry**

Test results from cone calorimetry yielded a large amount of useful data, such as heat release rate, heat of combustion, mass loss rate, specific extinction area, time to ignition, rate of production and yields of carbon monoxide and carbon dioxide.

Cone data was only obtained for the combustion of untreated and treated pine, as well as the pyrolysis of treated pine. Due to time and material constraints, testing of pyrolysis of untreated wood was unable to be carried out.

### 5.3.1 Mass Percent

Figure 33 shows the percentage of mass as a function of time for treated as well as untreated pine.

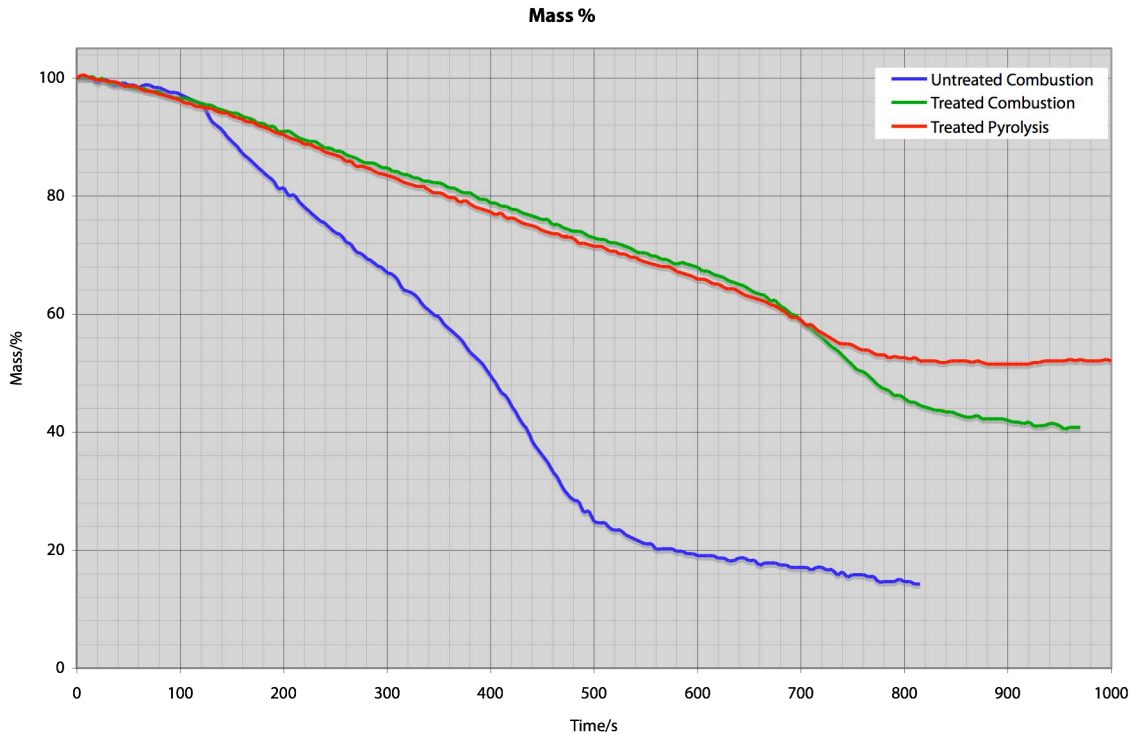


**Figure 33: Mass percent as a function of time**

From Figure 33 it can be clearly seen that fire retardant treatment has a large impact on how pine behaves under combustion and pyrolysis. The mass loss of both combustion and pyrolysis of treated pine can be observed as slow and steady for the majority of the time. Somewhat of a sharp decrease occurred before the mass loss leveled out. In the case of untreated pine, mass loss was rather steady, but much faster as observed by the high negative slope. The residual mass percent of both the treated specimens was more than 15% [of total mass] higher. This proved the efficiency of the fire retardant treatment in that a higher percentage of the sample's original mass was conserved after the burning process. After being

treated, as much as up to fifty percent of the original sample was still present, whereas only fifteen percent remained of the non-treated sample.

### 5.3.2 Mass Loss Rate

The MLR analysis of a sample can be useful since it can be used to locate the 'hot' areas where much of the mass is being lost. Figure 34 shows the mass loss rate curve for the three samples.

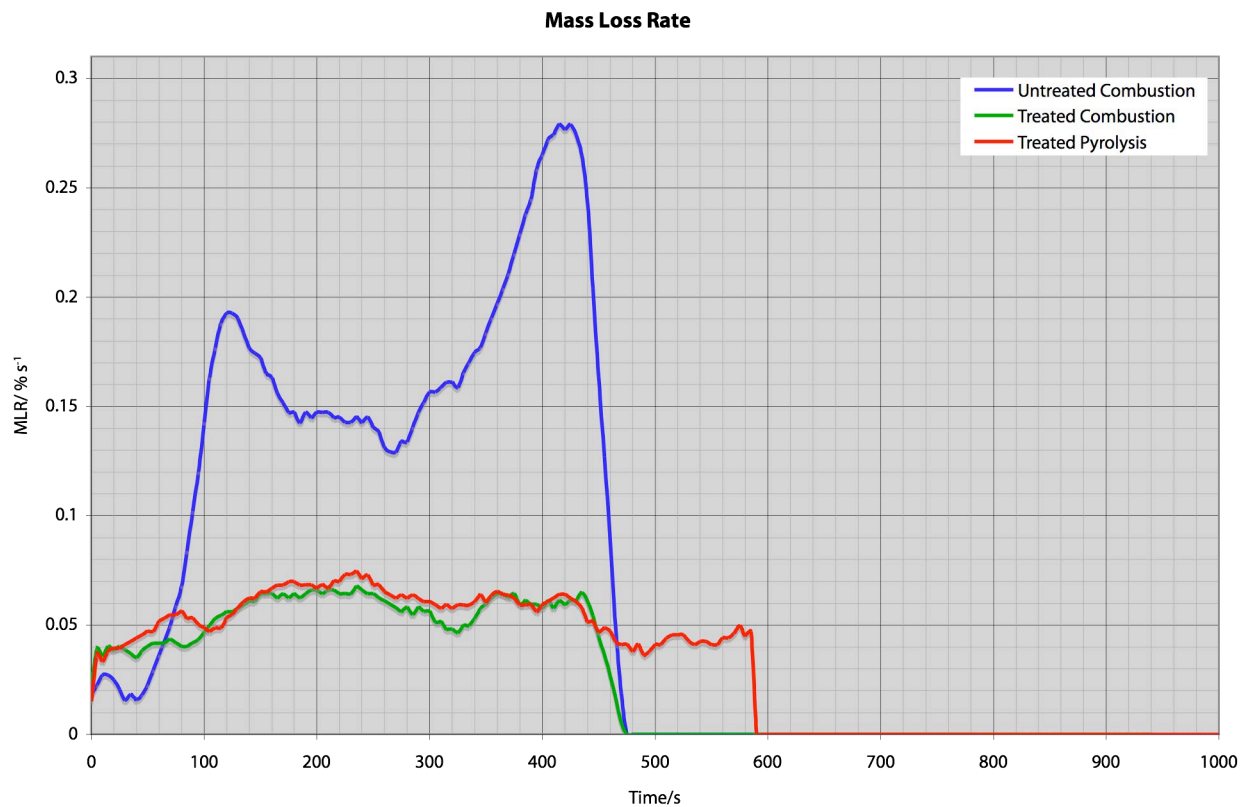


**Figure 34: Mass Loss Rate as a function of time**

Once again, a big divide was seen between the behavior of treated and untreated pine. For the untreated pine, it was clear that there were two points at which mass loss peaked: first around 120s, and then higher mass loss rate around 420s. This

contrasted with the treated pine, which for the most part seemed to display a relatively uniform rate of mass loss. Pyrolysis of treated pine also lasted around 115s longer than the two combustion runs, which both stopped around 480s.

The mass loss rate of the combustion of untreated pine once again occurred in a two-step process, as has been previously seen.

### **5.3.3 Heat Release Rate**

The heat release rate is a relatively simple indicator that can sum up the behavior of the sample. Combined with the peak heat release rate and the total heat release rate, this data can often be sufficient to grasp a basic understanding of a material. HRR curves are plotted in Figure 35.

Only the HRR during combustion were obtained from the cone data. The heat release rate during pyrolysis was so negligible that it was not detected. This concurred with findings published by CSIRO in the FWPRDC report of 2006.

The heat release rate for untreated combustion was similar as has been seen before, where pyrolysis associated with homogeneous combustion of volatile products was demonstrated by the first peak, and a decline in the HRR to a lower plateau where heterogeneous combustion occurred along with gasification of char (Kanury 1994). It was here where the volatiles may be contained within the pore structure of the char. As this char broke down and volatiles were released, a second peak developed as air and heat gained access to the remaining volatile material. This was followed by the curve descending once again, often to the baseline.

Treated pine on the other hand gave rise to only one peak around 740s, which was much later than the peaks found in the untreated samples. This behavior was

expected from the treated sample, as it did not ignite or release much heat until much later in the process.

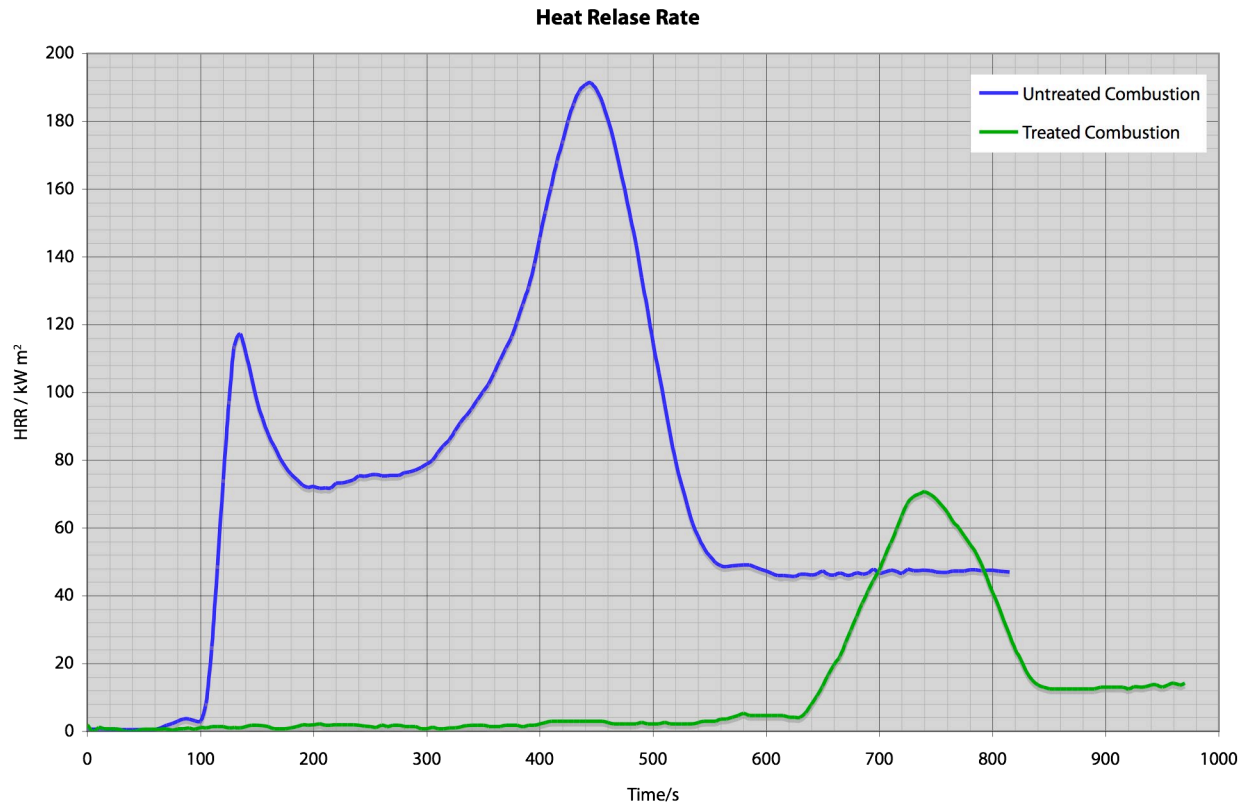


**Figure 35: Heat Release Rate as a function of time**

The total heat released by the treated sample in this test was 47 000 kW m<sup>-2</sup>, whereas the untreated sample had a total heat release of 8 550 kW, which was only 18% of the untreated sample.

The expected effectiveness of the treated sample could also be shown by comparing times to ignition. Untreated pine ignited within 115 s on average, whereas treated pine ignited well after 600 s on average.

### **5.3.4 Recommendations**

Several shortcomings were observed with the cone testing procedures. The following are some recommendations that can be implemented to improve the quality, reproducibility, and integrity of the results.

#### ***5.3.4.1 Sample Orientation***

Due to the granular structure of wood, its orientation with respect to the direction of the flame has a large impact on its behavior. Tran (1992) explored the effects of grain orientation in *Heat Release in Fires* and noted that it should be a factor that must be observed while testing with wood. Schaeffer (1967) also investigated charring in woods transverse to the grain and concluded it to be an important factor in the burning of wood. However, while cone testing was conducted no attention was paid to the grain orientation of the wood samples.

#### ***5.3.4.2 External Heat Flux***

Tran (1992) also referred to the importance of the external heat flux used. Material behavior changes drastically with different heat fluxes, and the most observable differences occur with lower heat fluxes. Even though several heat fluxes were tested during the pilot tests of this investigation, it might have been beneficial to consider a wider testing range.

### **5.3.4.3 Conditioning/Ambient Conditions**

Moisture content of wood is another very important factor that affects how it behaves. Tran (1992) went on to say, "It may be intuitively obvious that increasing the moisture content of material should act to reduce its HRR." This was one of the major setbacks encountered during the course of this project. Untreated and treated pine samples were prepared by an outsourced laboratory, where they had been properly conditioned to the right moisture content and temperature. However, upon receiving them in our lab, the same conditioning regimen was not followed. Unaware of the correct storage protocols, the samples were exposed to different ambient conditions before usage. This was realized much later during the testing phase, at which point it was too late to recondition the few remaining samples.

Nonetheless, to get an idea of the magnitude of the difference, the remaining samples were stored in a conditioning cabinet (at conditions specified by the manufacturer of the samples), and their masses were monitored over a period of ten days. It was found on average that an increase of 20% in mass was noted for all the samples. Due to the higher moisture content in the pine, an increase of ~25% was noted for ignition to occur for untreated pine. The samples used for the thermal analyses were taken before the realization that proper conditioning was required, which may have possibly affected some of that data.

## **5.4 TGA-DTA**

In this discussion, both the integral and the differential thermogravimetric curves are presented since both sets of curves contain important information that was useful in understanding the thermal behavior of the materials. In most of the DTG curves, a peak below 100°C was observed. This represented drying of the wood,

and the release of water vapor. However, it was the peaks at higher temperatures that represented the combustion and pyrolysis of the materials under investigation.

Figure 36-Figure 39 show the four TG plots, including all three heating rates.

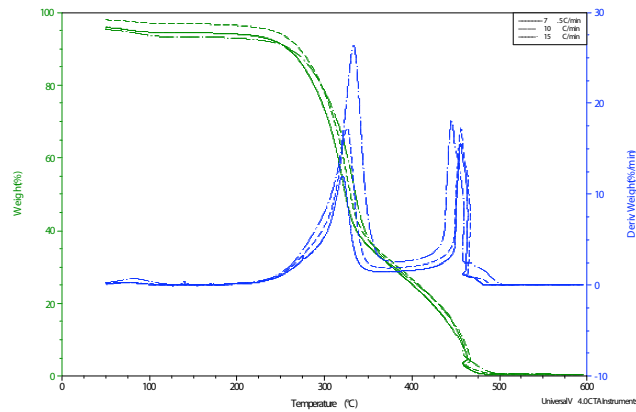


**Figure 36: Thermogravimetric plot for combustion of untreated pine**

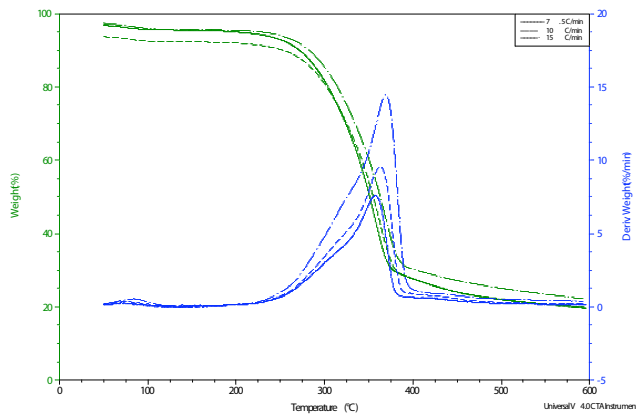


**Figure 37: Thermogravimetric plot for pyrolysis of untreated pine**

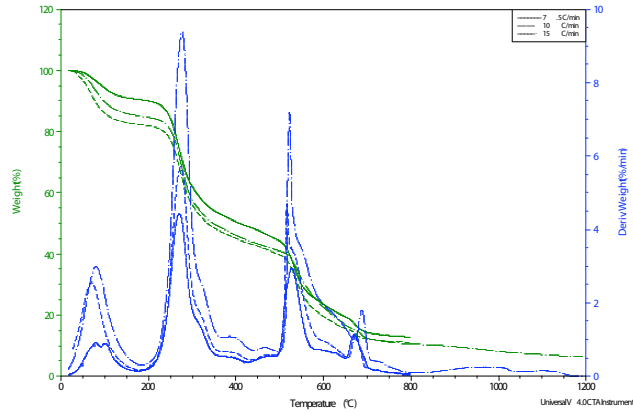


**Figure 38: Thermogravimetric plot for combustion of treated pine**

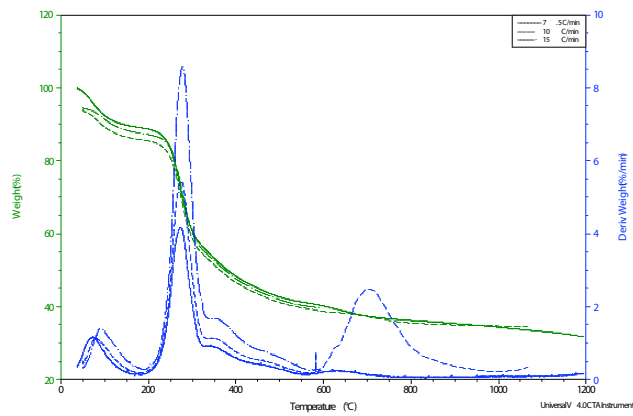


**Figure 39: Thermogravimetric plot for pyrolysis of treated pine**

### 5.4.1 Discussion of thermogravimetric analyses

Both pyrolysis and combustion mechanisms of wood, cellulose, hemicellulose, and lignin have been studied in great detail, leading to the rise of numerous theories and possible mechanisms. Of the three components that mainly comprise wood, cellulose thermally degrades through two types of reactions. At lower temperatures (200-280°C), there is a gradual degradation, which includes

depolymerization, hydrolysis, oxidation, dehydration, and decarboxylation. Carbon monoxide and carbon dioxide gases are also evolved, and carbonyl and carboxyl groups are formed, resulting in a carbonaceous residue. At higher temperatures (280-340°C), rapid volatilization occurs via the formation of laevoglucosan, leaving a charred residue. Laevoglucose decomposes into volatile and flammable products. These processes are shown schematically in Figure 41 (Kandola, et al 1996).

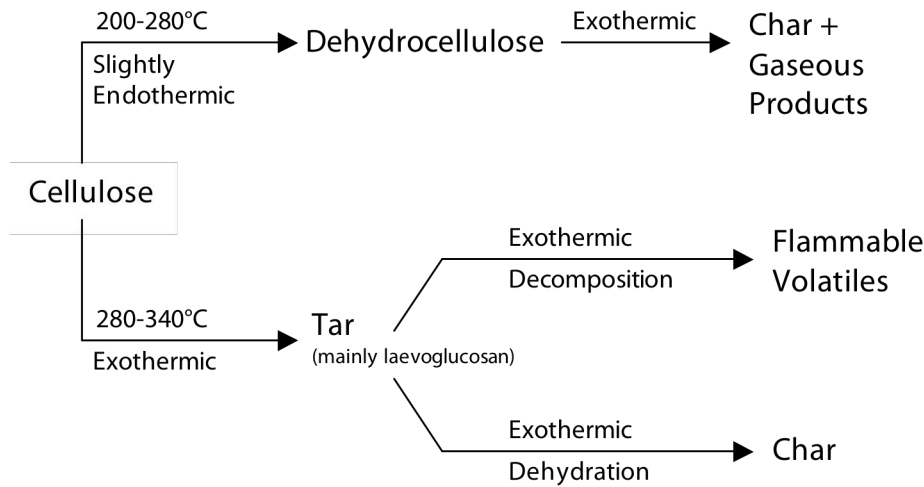


**Figure 41: Various stages in pyrolysis of cellulose**

Using this information, cellulosic pathways could be determined from the DTG data. Degradation of cellulose occurred around 320°C for the combustion of treated pine, as can be seen in Figure 36, meaning the exothermic formation of tar occurred in Phase I. Taking into consideration the FTIR data in Figure 27, it can be seen that gases were released subsequent to the formation of the laevoglucosan, which lead us to conclude that exothermic decomposition took place, releasing flammable volatiles in Phase II.

In the case of pyrolysis of untreated pine, Figure 37 shows the exotherm occurred around 360°C, once again leading us to believe that an exothermic process

occurred. However, we concluded that this was followed by exothermic dehydration leading to the formation of char. The char then acted as an insulator, preventing further degradation. This explains the presence of only one peak in the DTG.

From these thermal analyses of untreated pine, it is clear that oxidative decomposition of wood occurs at higher temperatures ( $>290^{\circ}\text{C}$ ), and the heat release is distributed between two sharp and relatively closely spaced exotherm, indicating a large rate of heat release. The heat liberated is easily transferred back to wood surfaces to continue the decomposition of wood, which maintains a continuous supply of gaseous fuel for flame propagation. This makes the wood catch fire easily and burn vigorously with a flame (Gao, et al 2004).

Looking at Figure 38, cellulosic degradation was observed in Phase II around  $275^{\circ}\text{C}$  during the combustion of treated pine. This could be attributed to the endothermic degradation of the cellulose present in the pine. The presence of a subsequent peak around  $500^{\circ}\text{C}$  (Phase III) further supported this conclusion, as gaseous products such as carbon dioxide and carbon monoxide were released (see Figure 30).

Lastly, from the pyrolysis of treated pine in Figure 39, an endotherm around  $285^{\circ}\text{C}$  which lead us to believe that endothermic cellulosic degradation occurred. Further supported by Figure 32, we saw gaseous products such as carbon monoxide and sulfur dioxide were evolved after dehydrocellulose degraded exothermically. It was also quite possible that a larger amount of char was formed than in the combustion of treated pine, leading to an endotherm of lower magnitude. The formation of char was an occurrence that the treated samples under both combustion and pyrolysis displayed. This is regarded as a good quality of a fire retardant since it is the char that insulates the rest of the wood from further

degradation, and in cellulosic materials the amount of char formation is increased at the cost of flammable volatile products by fire retardants (Gao, et al 2004).

According to Hirata and Kawamoto (1991), cellulose normally begins mass loss above 300°C, and most rapidly completes loss to yield the least amount of char, but the greatest amount of volatiles of all wood components. Lignin and hemicellulose on the other hand decompose with lower rates to produce greater quantities of char. The pyrolytic behavior of wood is the combined and overall behaviors of all three components, making it extremely complicated. However, it is proposed in the literature that of all of wood's components, it is cellulose that causes and seeds flaming combustion, and plays a key role in the pyrolysis because of its high pyrolysis rates (Gao, et al 2004). Gao (2003) further states that cellulose is probably exclusively responsible for the degradation of wood.

Liu (2003) suggested that comparing the first DTG peak to literature values, it is very likely that the controlling mechanism for the first step could be the pyrolysis of not only cellulose, but also that of hemicellulose and partly lignin pyrolysis. The second peak loss is likely to be due to combined effect of lignin pyrolysis in addition to the factors discussed previously. This evidence lead to the basic assumption of the dual phase kinetic model, where the two major mass losses were regarded as two independent reactions respectively occurring in the lower and higher temperature ranges.

#### **5.4.2 Discussion of Burn-X treated pine**

The exact mechanism by which salts and metal ions exercise their dramatic influence on the course of pyrolysis is not completely known (Antal and Varhegyi, 1995). There is some disparity over whether the effect of salts during cellulosic pyrolysis is catalytic in nature or not. Zaror (1982) has proposed that added

chemicals may undergo chemical reactions along stoichiometric lines, and that the type of reaction initiated affects the course of char forming reactions.

In 1991, Richards and Zheng postulated a stepwise mechanism from cellulose pyrolysis that placed a great amount of importance on inorganic compounds on the yield of laevoglucosan. Since pyrolysis reactions are a complex set of heterogeneous reactions occurring at high temperature, more than one type of chemical interaction between the inorganic salt and the organic molecules are likely to take place. Moreover, the very chemical and physical nature of the inorganic salt might determine its role during pyrolysis (Zaror 1982).

It is already known that fire retardants catalyze the formation of non-flammable char at the expense the production of flammable volatiles. Acid catalysts promote dehydration and favor formation of laevoglucosenone, furan derivative, dextrans, and tars. However, alkaline catalysts such as Burn-X enhance the fission and disproportionation reactions as evidenced in increased yields of glyoxal, acetaldehyde and other low-molecular weight carbonyl compounds, and char. The influence of catalysts on the pyrolysis process confirms the ionic nature of pyrolytic mechanisms (Beaumont & Schowb 1984).

Potassium, lithium, and calcium ions strongly promote the formation of char from wood at the expense of tar (and laevoglucosan) formation. Other metal ions such as iron and copper enhance the yield of laevoglucosan and char from wood (Richards & Zheng 1991).

It has also been suggested that chlorine radicals ( $\text{Cl}\bullet$ ) form in thermal decomposition as radical scavengers block the formation of volatile flammable products (Xu, et al 2002). This leads to a lower weight loss and a smaller exotherm owing to oxidation of volatile products. Furthermore, the hydrogen chloride

released exerts further effect by catalyzing the dehydration, condensation, and charring reactions.

## 6 Conclusions

The purpose of this investigation was to better understand the fire retardant process by considering the two systems of untreated pine and Burn-X treated pine, by attempting to deconstruct the process by quenching the devolatilization at various stages. This would allow us to closely examine the decomposition process and gain insight into the mechanism of char formation and its subsequent collapse, which would allow us to make a contribution to the physico-chemical mechanism of devolatilization for wood.

Unfortunately, the volumetric sorption analyzer to be used for measuring char surface area and pore measurements was unavailable; hence, no data regarding char formation was collected. Nevertheless, data was collected and used from the cone calorimeter as well as from the differential thermogravimetric apparatus, and infrared spectrometer, which even though was not substantial to fully understand the physico-chemical mechanisms of degradation of wood, gave a sense of the processes.

Kinetic parameters such as the activation energy and pre-exponential factor were evaluated using TGA-DTGA data. These data supported the premise that the degradation of wood occurred in two phases, where the first peak was caused by the pyrolysis associated with homogenous combustion of volatile products, and the second peak resulted from the heterogeneous combustion with the gasification of char. For a heating rate of  $10^{\circ}\text{C min}^{-1}$ , activation energies for combustion of treated wood were  $28.5 \text{ kJ mol}^{-1}$  between  $205\text{-}340^{\circ}\text{C}$ ,  $28.4 \text{ kJ mol}^{-1}$  between  $490\text{-}660^{\circ}\text{C}$ , and  $25.2 \text{ kJ mol}^{-1}$  between  $660\text{-}700^{\circ}\text{C}$ . For the pyrolysis of treated pine, activation energies were found to be  $28.5 \text{ kJ mol}^{-1}$  over  $190\text{-}340^{\circ}\text{C}$ , and  $3.1 \text{ kJ mol}^{-1}$  between  $570\text{-}930^{\circ}\text{C}$ . Combustion of untreated pine yielded activation energies of  $70.0 \text{ kJ mol}^{-1}$  between  $225\text{-}375^{\circ}\text{C}$ , and  $30.5 \text{ kJ mol}^{-1}$  between  $375\text{-}460^{\circ}\text{C}$ .

The pyrolysis of untreated pine had an activation energy of  $49.8 \text{ kJ mol}^{-1}$  over a temperature range of 225-400°C.

From the infrared spectroscopy, it was generally found that the evolution of gases peaks coincided with peaks in mass loss rate, which added to the knowledge of how the wood degraded in each situation. The combustion of treated pine mainly yielded the evolution of large amounts of carbon dioxide, followed by smaller quantities of sulfur dioxide and carbon monoxide. Likewise, the combustion of untreated pine also led to the gaseous release of mainly carbon dioxide, followed by smaller quantities of carbon monoxide and sulfur dioxide. The pyrolysis of treated pine saw the evolution of mainly sulfur dioxide, and smaller quantities of carbon dioxide, carbon monoxide, and methane. Sulfur dioxide was the gas given off in the largest quantity during pyrolysis of untreated pine, followed by that of carbon dioxide, carbon monoxide, ethylene, methane, and ethane.

In conclusion, even though relationships between the development of char and porosity in degradation of wood were not established, the effects of a fire retardant additive upon the degradation mechanisms were better understood. It can be concluded that Burn-X is an acceptable fire retardant treatment given its low total heat release rate, delayed ignition times, and low probability of flame sustenance. In addition, it also made the wood decompose at an initially lower temperature where cellulose, the critical component in wood, decomposed through endothermic degradation, producing large amounts of insulating char and correspondingly less amounts of flammable volatiles (Gao, et al 2004).

## 7 References

"The Chemistry of Pyrolysis and Combustion." Advances in Chemistry Series 207. Chem. Solid Wood (1984): 489.

Alaee, M., Arias, P., Sjodin, A., and Bergman, A. "An overview of commercially used brominated flame retardants, their applications, their use patters in different countries/regions and possible modes of release." Environmental International 29. (2003).

Alén R. "Structure and Chemical Composition of Wood." Forest Products Chemistry, Papermaking Science and Technology Book, 3<sup>rd</sup> edition. Stenius, Fapet Oy, Finland. (2000).

Babrauskas, V. "Ignition of Wood. A review of the state of the art." Interflam 2001. Interscience Communications Ltd., London (2001).

Babrauskas, Vytenis, and S. J. Grayson. Heat Release in Fires. New York, NY, USA: Elsevier Applied Science; Elsevier Science Pub. Co.,1992.

Birky, M. M. Polymer Prepr. 14.2 (1973):1011-1015.

Bourgois, J. and Guyonnet, R. "Characterization and analysis of torrefied wood." Wood Science and Technology 22 (1988).

Branca, Carmen, Di Blasi, Colomba. "Global Kinetics of Wood Char Devolatilization and Combustion." Energy and Fuels 17 (2003):1609-1615.

Broido, A. "A Simple, Sensitive Graphical Method of Treating Thermogravimetric Analysis Data." Journal of Polymer Science, Part A-2 7 (1969):1761-1773

Byrne, G.A. et al. "The Pyrolysis of Cellulose and the Action of Flame-Retardants. II- Further Analysis and Identification of Products." J. Appl. Chem. 16 (1966).

C.A. Zaror. "Studies of the pyrolysis of wood at low temperatures." Department of Chemical Engineering and Chemical Technology, Imperial College, London (1982).

de Wit, C.A. "An overview of brominated flame retardants in the environment." Chemosphere 46 (2002).

Einhom, I. N., M. M. Birky, M. L. Grunnet, S. C. Packham, J. H. Petajan, and J. D. Seader "The physiological and toxicological aspects of smoke produced during the combustion of polymeric materials." Annual report 1973-1974. UTEC-MSE 74-060, FRC/UU26. Univ. of Utah, Salt Lake City, Utah (1974).

Fang, J.B. "Wood Fire Behaviour and Fire Retardant Treatment: A Review of the Literature." Ignition Properties of Cellulose Materials: A Survey of the Literature. Canadian Wood Council, Ottawa. (1966).

M.X. Fang, D.K. Shen, Y.X. Li, C.J. Yu, Z.Y. Luo, K.F. Cen. "Kinetic Study on Pyrolysis and Combustion of Wood Under Different Oxygen Concentrations by using TG-FTIR Analysis." Journal of Analytical and Applied Pyrolysis 77 (2006): 22-27.

Forest Products Laboratory, and Inc Building News. Wood Engineering Handbook. Anaheim: BNI Building News, 2000.

Gao, M., Sun, C., Zhu, K. "Thermal Degradation of Wood Treated with Guanidine Compounds in Air." Journal of Thermal Analysis and Calorimetry 75 (2004):221-232

G.N. Richards, G. Zheng. J. Anal. Appl. Pyrolysis 21 (1991): 133 – 146.

Grassie, N. and Scott, G. Polymer Degradation and Stabilisation. Cambridge University Press, New York (1985).

- H. Y. Shi. "Kinetic Study of Fire Combustible Pyrolysis". Zhejiang University, Hangzhou. (2004): 20-21.
- Holmes, Carlton A. "Effect of Fire-Retardant Treatments on Performance Properties of Wood." United States Department of Agriculture, Wisconsin. (1977).
- Holmes, Carlton A. "Effect of Fire-Retardant Treatments on Performance Properties of Wood." ACS Symposium Series 43. Wood Technology: Chem. Aspects, Symp. (1977): 82.
- "Rate of Heat Release Measurement using the Cone Calorimeter." Journal of Thermal Analysis 35.6 (1989): 1861.
- J. Rath, G, Staudinger. Fuel 80 (2001): 1379-1389.
- Kandola, B.K., Horrocks, A.R. "Flame-Retardant Treatments of Cellulose and Their Influence on the Mechanism of Cellulose Pyrolysis." Rev. Macromol. Chem. Phys. C346.4 (1996):721-794
- Kanury, A. M. "Combustion characteristics of biomass fuels." Combust. Sci. Technol. (1994): 97, 469-491.
- KISSC NUANCE. "Keck-II – What is FT-IR?" Northwestern University 2006. <<http://www.nuance.northwestern.edu/KeckII/ftir1.asp>>.
- Kozłowski R. and Władysław-Przybylak M. "Natural polymers, wood, and lignocellulosic materials." Fire Retardant Materials. Woodhead Publishing Limited, Cambridge, England. (2001).
- Kuryla, W.C., and Papa, A.J. Flame Retardance of Polymeric Material 4. Marcel Decker Inc, New York. (1978).
- Larson, E.R. Fire and Flammability / Flame Retardant Chemistry 1 & 4. (1974).

- LeVan, S.L. and Winnandy, J.E. "Effects of Fire Retardant Treatments on Wood Strength: A Review." Wood and Fiber Science 22 (1990).
- Liu, Naian, et al. "Kinetic Compensation Effect in Thermal Decomposition of Cellulosic Materials in Air Atmosphere." Journal of Applied Polymer Science 89.1 (2003): 135-141.
- M. Gao, D. X. Pan, and Y. C. Sun. Journal of Fire Science 21 (2003): 189.
- M.J. Antal Jr, G. Varhegyi. Ind. Eng. Chem. Res. 34 (1995):703 – 717.
- Meier, D. and Faix, O. "State of the Art of Applied Fast Pyrolysis of Lignocellulosic Materials – A Review." Bioresource Technology 68. (1999).
- Miller, R.B. "Structure of Wood." Wood Handbook – Wood as an Engineering Material. United States Department of Agriculture Forest Service, Forest Products Laboratory, Madison WI (1999).
- O. Beaumont, Y. Schwob. Ind. Eng. Chem. Proc. Des. Dev. 23 (1984): 637 – 641.
- O'mara, M. M. J. Fire & Flammability 5.1 (1974):34-53.
- Orfão, J. J. M., F. J. A. Antunes, and J. L. Figueiredo. "Pyrolysis Kinetics of Lignocellulosic materials—three Independent Reactions Model." Fuel 78.3 (1999/2): 349-58.
- Parham, R.A. and Gray, R.L. "Formation and Structure of Wood." The Chemistry of Solid Wood, Advances in Chemistry Series 27. American Chemical Society, Washington, DC. (1984).
- Rahman, F., Langford, K.H., Scrimshaw, M.D., and Lester, J.N. "Polybrominated diphenyl ether (PBDE) flame retardants." Science of the Total Environment. (2002).
- Robison, M. M., P. E. Wagner, R. M. Fristrom, A. G. Schulz. Fire Technol. 8.4 (1972): 278-

290.

- Roberts, A.F. "A review of kinetics data for the pyrolysis of wood and related substances." Combustion and Flame 14.2 (1970):261-272.
- Rowell, R.M. "Penetration and Reactivity of Cell Wall Components." The Chemistry of Solid Wood, Advances in Chemistry Series 27. American Chemical Society, Washington, DC. (1984).
- Sanne Dolmer, iNano. Denmark 2006. <<http://www.inano.dk/sw256.as>>.
- Schaffer, E. L. Charring Rate of Selected Woods—Traverse to Grain. Madison: Wis., U.S. Dept. of Agriculture, 1967.
- "Study on the Fire Retardant Mechanism of Fire-Retardant FRW by FTIR." Scientia Silvae Sinicae 41.4 (2005): 149.
- Shafizadeh, F. "The Chemistry of Pyrolysis and Combustion." The Chemistry of Solid Wood, Advances in Chemistry Series 207. American Chemical Society, Washington, DC. (1984).
- Sharatov, Kfir. "Thermo gravimetric analyzer (TGA) and differential scanning calorimeter (DSC) for materials lifetime studies." 2001. <<http://www.tau.ac.il/~shapiray/MResearchF.htm>>.
- T. Hirata, and S. Kawamoto. Fire Materials (1991): 27.
- Tang, W. K., and H. W. Eickner. U.S. Forest Service Research Paper FPL 82 (1968)
- Tran, Hao C. "Experimental Data on Wood Materials." (1992).
- Tran, Hao C. "Rates of Heat and Smoke Release of Wood in an Ohio State University Calorimeter." Fire and Materials 12.4 (1988): 143.

Troitsch, J. H. "Overview of Flame Retardants." 1998. <[http://www.bsef-site.com/science/over\\_fr.pdf](http://www.bsef-site.com/science/over_fr.pdf)>.

Troitsch, J.H. Plastics Flammability Handbook. Hanser Gardner Publications, Inc., Munich. (2004).

Wagner, J. P. Fire Res. Abstr. and Rev. 14.1 (1972): 1-23.

Wang, Qingwen, Li, Jian, and Winandy, Jerrold E. "Chemical mechanism of fire retardance of boric acid on wood." Research Institute of Wood Science and Technology, Harbin, China. (June 2004).

White, R.H. and Dietenberger, M.A. "Wood products: thermal degradation and fire." Encyclopedia of Materials: Science and Technology. Elsevier Science Ltd. (2002).

Wilkins, E., and F. Murray. "Toxicity of Emissions from Combustion and Pyrolysis of Wood." Wood Science and Technology 14.4 (1980): 281.

Winandy, J.E. and Rowell, R.M. "The Chemistry of Wood Strength." The Chemistry of Solid Wood, Advances in Chemistry Series 207. American Chemical Society, Washington, DC. (1984).

Xu, J.Z., Gao, M., Guo, H.Z., Liu, X.L., Li, Z., Wang, H., Tian, C.M. "Study on the Thermal Degradation of Cellulosic Fibers Treated with Flame Retardants." Journal of Fire Sciences 20 (2002):227-235.

# Appendix A – Burn-X™ MSDS



## Material Safety Data Sheet

1. Description	
<b>Product Name</b>	Burn-X
<b>Product Use</b>	Flame retardant, insecticide and fungicide for cellulose based materials
<b>Manufacturer</b>	Vega Kimya Ltd. Mecidiye Cad. 36/6, Kristal Apt 34457 Tarabya/Istanbul, Türkiye Tel: 0090 212 299 89 10 Fax: 0090 533 942 72 09 <a href="http://www.burn-x.com">www.burn-x.com</a> <a href="http://www.vega-ltd.com">www.vega-ltd.com</a> email: <a href="mailto:info@vega-ltd.com">info@vega-ltd.com</a>

## 2. Ingredients

Ingredients	CAS#	Wt%	ACGIH-TLV	LC50	LD50
Water	7732-18-5	>30	N/A	N/A	14.500 mg/kg oral, rat
Natural Minerals	N.D.	>30	N/A	N/A	14.800 mg/kg oral, rat

PH (unit)	9,40
Conductivity	330000 umhos/cm
Saltines	% 00 200
Total solid material	375,5 g/L
Solid material	5,78 g/L
Total hardness	26000 F
Calcium Ion	100 g/L
Magnesium Ion	1,2 g/L
Sodium Ion	2,8 g/L
Potassium Ion	2,6 g/L
Chloride Ion	185 g/L
Sulphate Ion	0,25 g/L
Bicarbonate Ion	0,2 g/L
Carbonate Ion	0,1 g/L
Barium	0,22 mg/L

## 3. Physical/Chemical Characteristics

<b>Boiling Point</b>	108 ° C
<b>Vapour Pressure (mm Hg):</b>	Not available
<b>Vapour Density (Air=1)</b>	>1
<b>Solubility in Water:</b>	Complete
<b>Specific Gravity (H2O=1)</b>	1,169
<b>Evaporation Rate</b>	Not available
<b>Appearance &amp; Odour</b>	Clear, colourless, no odour
<b>% Volatile (Wt %)</b>	Not available
<b>Evaporation Rate (Water=1)</b>	Not available
<b>pH</b>	9,40
<b>Viscosity</b>	1,05 mPas
<b>Ash Content</b>	35 %
<b>Odour Threshold (ppm)</b>	Not available

## 4. Fire/Explosion Data

<b>Flammability</b>	Not flammable
---------------------	---------------

<b>Flash Point</b>	Not available
<b>Hazardous Combustion</b>	Not available
<b>Products</b>	
<b>Autoignition Temperature</b>	Not available
<b>Extinguishing Media</b>	Self extinguisher
<b>Special Firefighting Procedures</b>	Not necessary, as product is natural fire retardant
<b>Unusual Fire % Explosion Hazards</b>	None known
<b>5. Reactivity Hazard Data</b>	
<b>Chemical Stability</b>	Stable
<b>Incompatible Materials</b>	Oil based chemicals
<b>Reactivity</b>	Not available
<b>Hazardous Decomposition Products</b>	Not decomposable
<b>6. Health Hazard Data</b>	
<b>Route of Entry</b>	Ingestion
<b>Acute Exposure</b>	Eye: no irritation Ingestion: no irritation
<b>Chronic Exposure</b>	None known
<b>Irritancy</b>	Non hazardous
<b>Carcinogenicity</b>	Non hazardous by WHMIS/OHSA criteria
<b>Teratogenicity</b>	No data available
<b>Mutagenicity</b>	No data available
<b>Synergistic Materials</b>	Not available
<b>7. Preventative Measures</b>	
<b>Gloves</b>	No recommendation
<b>Eye Protection</b>	Not normally required
<b>Resp. Protection</b>	Not normally required
<b>Other Protective Equipment</b>	As required by employer code
<b>Engineering Controls</b>	General ventilation normally adequate
<b>Leak &amp; Spill</b>	Before attempting clean up, refer to hazard data given above. Small spills may be absorbed with non reactive absorbent and placed in suitable, covered, labeled containers. Prevent large spills from entering sewers or waterways. Contact emergency services and supplier for advice.
<b>Waste disposal</b>	Review federal, provincial and local government requirements prior to disposal
<b>Storage &amp; Handling</b>	Keep out of reach of children. Store in closed container away from incompatible materials.
<b>8. First Aid</b>	
<b>Eye</b>	Not a normal route of harmful exposure. Flush with water. Remove contact lenses, if applicable and continue flushing. Obtain medical attention if irritation develops.
<b>Skin</b>	Not a normal route of harmful exposure. Flush with water. Wash with soap and water. Obtain medical attention if irritation develops.
<b>Inhalation</b>	Not a normal route of harmful exposure. If symptoms develop, move to fresh air. If symptoms persist, obtain medical attention.
<b>Ingestion</b>	Do not induce vomiting. Rinse mouth with water, and then drink one glass of water. Obtain medical attention.
<b>9. Preparation Information</b>	
	Date: 20th March, 2004 MSDS Prepared By: Vega Kimya Ltd.